



Sweden
Sverige



SOURCE APPORTIONMENT STUDY FOR KAVADARCI URBAN AREA



GOCE DELCEV
UNIVERSITY
FACULTY OF NATURAL
AND TECHNICAL SCIENCES

AMBICON.UGD

This study was prepared by the AMBICON laboratory at Goce Delcev University—Stip as part of the "Scaling-up Actions to Tackle Air Pollution" project, which is implemented by the United Nations Development Programme (UNDP) in partnership with the Ministry of Environment and Physical Planning, along with the municipalities of Kavadarci, Kumanovo, Gostivar, Struga, and Strumica.

The project is a component of the UNDP Framework Programme funded by Sweden. The Programme also includes the project "Building municipal capacities for project implementation".

The views expressed in this study are those of the author and do not necessarily reflect the views of the UNDP, Sweden as the donor, or the other project partners.

Document title:	Source Apportionment Study for Kavadarci urban area
Name of the organization:	University Goce Delcev, Stip, AMBICON Lab – Faculty of Natural and Technical Sciences
Country	Republic of North Macedonia
Project title:	Scaling-up actions to tackle air pollution
Project Number:	00122883
Submitted To:	UNDP, Skopje
Date of submission	03.04.2025
Project team	
Team leader	Prof. Dr. Dejan Mirakovski – UGD FNTS
Chemical speciation and modelling	Ass. Prof. Dr. Afrodita Zendelska – UGD FNTS
QA/QC group	Prof. Dr. Marija Hadzi-Nikolova – UGD FNTS Prof. Dr. Blazo Boev – UGD FNTS
Laboratory process support	Prof. Dr. Tena Sijakova-Ivanova – UGD FNTS Ass. Prof. Dr. Ivan Boev – UGD FNTS Prof. Dr. Sonja Lepitkova – UGD FNTS Ass. Prof. Dr. Gorgi Dimov – UGD FNTS Ass. M.Sc. Ana Mihailovska – UGD FNTS
Technical group	M.Sc. Boban Samardziski, FNTS, AMBICON Igor Pavlov – FNTS, AMBICON Goce Bogatinov – UGD IT SG
Students' internship	Ana Marija Kostadinova
UNDP	Armen Grigoryan, Resident Representative Aleksandra Dimova Manchevska, Project Manager Dren Nevezati, Monitoring Associate Trajancho Naumovski, Project Assistant
Knowledge management and capacity building support	M.Sc. Pavlina Zdraveva
Communication support team	Igor Stojanov Elena Doneva

Contents

List of figures.....	4
List of tables.....	5
Symbols and abbreviations.....	5
Terms and definitions	6
1. Introduction	8
2. Background information's	9
2.1. Kavadarci urban area	9
2.2. Climate	10
2.3. Transportation and energy infrastructure	11
2.4. Industry and service providers.....	12
2.5. Historical data on ambient air quality	13
3. Major emission sources.....	16
3.1. Emissions inventory.....	16
3.2. Source profiles	17
4. Particulate matter sampling and analysis	22
4.1. Sampling and determination of mass concentration of ambient particulate matter (PM _{2.5})	22
4.2. Chemical speciation.....	25
4.3. Observations and results	29
Statistical Evaluation	29
5. Positive Matrix Factorisation	36
5.1. Input data and PMF model setting	38
5.2. Factor attribution to sources	38
5.3. Sources Contribution.....	43
6. Conclusions and recommendations	46
Lessons learned	48
References.....	49

List of figures

Figure 1. Map of municipalities included in this study	8
Figure 2. Location of Municipalities of Kavadarci [1]	9
Figure 3. Kavadarci topography map [2]	10
Figure 4. Maximum and minimum temperature maps for North Macedonia with probability of occurrence of 0,002% (Source: Climate maps, UHMR, 2020).....	10
Figure 5. Seasonal wind roses during the monitoring period (March 2023 to February 2024, AMBICON Lab).....	11
Figure 6. Number of registered vehicles in Kavadarci classified according to the type and fuel used	12
Figure 7. Sites with industrial infrastructure with IPPC (A and B category) permits [1].....	12
Figure 8. Service providers within Kavadarci urban area [1].....	13
Figure 9. Average annual concentration of SO ₂ from 2017 to 2021 [1]	13
Figure 10. Average annual concentrations of NO ₂ from 2019 to 2023 [1]	14
Figure 11. Maximum 8-hour averages of CO from 2018 to 2021 [1]	14
Figure 12. Maximum 8-hour averages of O ₃ from 2018 to 2021 [1].....	15
Figure 13. Average annual PM10 concentrations and frequency of exceedances of the 24-hour limit value.....	15
Figure 14. Sectoral contribution to particulate matter emissions	17
Figure 15. Woodstove burning chemical profile (closed fireplace).....	18
Figure 16. Open burning of crop residues chemical profile.....	18
Figure 17. Construction activities chemical profile	19
Figure 18. Exhaust diesel and gasoline chemical profile	19
Figure 19. Urban traffic chemical profile	19
Figure 20. Road dust chemical profile	20
Figure 21. Soil dust chemical profile	20
Figure 22. Residual oil chemical profile.....	21
Figure 23. Fuel oil chemical profile	21
Figure 24. Monitoring location in Kavadarci urban area	22
Figure 25. Sequential sampling system PNS 18T-DM 6.1.....	23
Figure 26. Weighing room- AMBICON UGD Lab	24
Figure 27. NEX CG by Rigaku.....	26
Figure 28. Spectroquant® Prove 600, Merck.....	28
Figure 29. Magee Scientific, SootScan™ Model OT21 Optical Transmissometer	29
Figure 30. PM 2.5 – daily average concentrations from March 2023 to March 2024	32
Figure 31. Daily variations in concentrations throughout all days, seasons, and weekdays	33
Figure 32. Bi-variate (seasonal), CPF and non parametric polar plots	33
Figure 33. Major components and elemental groups identified	34
Figure 34. Contribution of major particulate matter components [20, 21].....	35
Figure 35. Average monthly concentrations of lead (Pb) and nickel (Ni) in Kavadarci	35
Figure 36. Free software US-EPA PMF 5.0 version 5.0.14 – splash screen	37
Figure 37. Factor fingerprint for Kavadarci	39
Figure 38. Biomass burning factor profiles in Kavadarci	39
Figure 39. Traffic associated factors for Kavadarci dataset	40
Figure 40. Fuel and residual oil factor profiles	41
Figure 41. Mineral dust factor profiles	42
Figure 42. Open fire burning factor profile	42
Figure 43. Secondary Aerosols factor profile	43
Figure 44. Average monthly contributions to total particulate mass (PM 2.5) – Kavadarci	43

Figure 45. Relative monthly contribution – Kavadarci.....	44
Figure 46. Relative annual contribution of PM 2.5 sources at Kavadarci.....	45

List of tables

Table 1. Criteria pollutants emissions (in tons per year) for Kavadarci municipality [1]	16
Table 2. Quality control results of EDXRF NEX CG by Rigaku	26
Table 3. Zeta-score results of EDXRF inter-laboratory comparison	27
Table 4. Quality control results for water soluble ions standard operating procedure.....	28
Table 5. Statistical evaluation – Kavadarci dataset	29
Table 6. Corelation matrix – Kavadarci dataset	31

Symbols and abbreviations

For the purposes of this document, the following symbols and abbreviated terms apply.

- C Concentration of PM ($\mu\text{g}/\text{m}^3$) at ambient conditions
- GUM Guide to the Expression of Uncertainty in Measurement
- JCGM Joint Committee for Guides in Metrology
- PM Particulate Matter
- PTFE Polytetrafluoroethylene
- QA/QC Quality Assurance / Quality Control
- NIST National Institute of Standards and Technology
- QCS Quality Control Sample
- AQIP Academic Quality Improvement Plan
- EEA European Environment Agency
- TSP Total suspended particles
- NMVOC Non-methane volatile organic compounds
- MOEPP Ministry of environment and physical planning
- ED-XRF Energy dispersive X-ray fluorescence
- IC Ion chromatography
- OC Organic carbon
- EC Elemental carbon
- SA Source apportionment
- SD Standard deviation
- C.V. Coefficient of variation

Terms and definitions

For the purposes of this document, the following terms and definitions apply.

Ambient air – is outdoor air in the troposphere, excluding workplaces as defined by Directive 89/654/EEC [12] where provisions concerning health and safety at work apply and to which members of the public do not have regular access.

Calibration - operation that, under specified conditions, in a first step, establishes a relation between the quantity values with measurement uncertainties provided by measurement standards and corresponding indications with associated measurement uncertainties and, in a second step, uses this information to establish a relation for obtaining a measurement result from an indication.

Calibration Standard (CAL) - a solution prepared from the stock standard solution(s) which is used to calibrate the instrument response with respect to analyte concentration.

Certified reference material (CRM) is defined as a “reference material characterized by a metrologically valid procedure for one or more specified properties, accompanied by a reference material certificate that provides the value of the specified property, its associated uncertainty, and a statement of metrological traceability”.

Combined standard uncertainty - standard uncertainty of the result of a measurement when that result is obtained from the values of a number of other quantities, equal to the positive square root of a sum of terms, the terms being the variances or covariances of these other quantities weighted according to how the measurement result varies with changes in these quantities.

Coverage factor - numerical factor used as a multiplier of the combined standard uncertainty in order to obtain an expanded uncertainty.

Expanded uncertainty - quantity defining an interval about the result of a measurement that may be expected to encompass a large fraction of the distribution of values that could reasonably be attributed to the measurand.

Field blank - filter that undergoes the same procedures of conditioning and weighing as a sample filter, including transport to and from, and storage in the field, but is not used for sampling air, and it has the same treatment as samples.

Instrument Detection Limit (IDL) - the concentration equivalent of the analyte signal, which is equal to three times the standard deviation of the blank signal at the selected analytical mass(es).

Internal Standard - pure analyte(s) added to a solution in known amount(s) and used to measure the relative responses of other method analytes that are components of the same solution. The internal standard must be an analyte that is not a sample component.

Laboratory Reagent Blank (LRB) (Preparation Blank) - an aliquot of reagent water that is treated exactly as a sample including exposure to all labware, equipment, solvents, reagents, and internal standards that are used with other samples. The LRB is used to determine if method analytes or other interferences are present in the laboratory environment, the reagents or apparatus.

Linear Dynamic Range (LDR) - the concentration range over which the analytical working curve remains linear.

Limit value - level fixed based on scientific knowledge, with the aim of avoiding, preventing or reducing harmful effects on human health and/or the environment, to be attained within a given period and not to be exceeded once attained.

Method Detection Limit (MDL) - the minimum concentration of an analyte that can be identified, measured and reported with 99% confidence that the analyte concentration is greater than zero. MDLs are intended as a guide to instrumental limits typical of a system optimized for multi-element determinations and employing commercial instrumentation and pneumatic nebulization sample introduction. However, actual MDLs and linear working ranges will be dependent on the sample matrix, instrumentation and selected operating conditions.

Performance characteristic - one of the parameters assigned to a sampler to define its performance.

Performance criterion - limiting quantitative numerical value assigned to a performance characteristic, to which conformance is tested.

Period of unattended operation - time over which the sampler can be operated without requiring operator intervention.

PM_x - particulate matter suspended in air which is small enough to pass through a size-selective inlet with a 50 % efficiency cut-off at $x \mu\text{m}$ aerodynamic diameter.

Quality Control Sample (QCS) - a solution containing known concentrations of method analytes which is used to fortify an aliquot of LRB matrix. The QCS is obtained from a source external to the laboratory and is used to check laboratory performance.

Reference method (RM) - measurement method(ology) which, by convention, gives the accepted reference value of the measurand.

Sampled air - ambient air that has been sampled through the sampling inlet and sampling system.

Sampling inlet - entrance to the sampling system where ambient air is collected from the atmosphere.

Standard uncertainty - uncertainty of the result of a measurement expressed as a standard deviation.

Stock Standards Solutions - a concentrated solution containing one or more analytes prepared in the laboratory using assayed reference compounds or purchased from a reputable commercial source.

Suspended particulate matter - notion of all particles surrounded by air in a given, undisturbed volume of air.

Tuning Solution - a solution used to determine acceptable instrument performance prior to calibration and sample analyses.

Time coverage - percentage of the reference period of the relevant limit value for which valid data for aggregation have been collected.

Uncertainty (of measurement) - parameter associated with the result of a measurement that characterizes the dispersion of the values that could reasonably be attributed to the measurand

Weighing room blank - filter that undergoes the same procedures of conditioning and weighing as a sample filter, but is stored in the weighing room

1. Introduction

The "Scaling-up actions to tackle air pollution" project is a component of the UNDP Framework Programme, funded by Sweden. The project is being executed in North Macedonia by the United Nations Development Program (UNDP), in partnership with the Ministry of Environment and Physical Planning, as well as the municipalities of Gostivar, Kavadarci, Kumanovo, Struga, and Strumica.

Building on the results and lessons learned from the first phase conducted in Skopje, the project aims to scale up and replicate the developed concept in five additional cities facing air pollution challenges: Gostivar, Kavadarci, Kumanovo, Struga, and Strumica. Following the successful completion of the Source Apportionment Study for the City of Skopje, the AMBICON Laboratory has been tasked with preparing the Source Apportionment Studies for the five new municipalities: Gostivar, Kavadarci, Kumanovo, Struga, and Strumica.

The primary objective of a source apportionment study is to collect insights regarding pollution sources and their contributions to ambient air pollution levels. This information is essential for developing effective air quality policies, which are necessary for the implementation of the Air Quality Directives (Directive 2008/50/EC and Directive 2004/107/EC).

The actions undertaken followed the rigorous study approach outlined in the European guide on air pollution source apportionment with receptor models (Revised edition 2019, JRC) and included:

- Preliminary evaluation of areas under examination (emission inventories, time series of pollutants and meteorology etc),
- Selection of representative receptors/monitoring sites,
- Sampling and chemical speciation,
- Construction of multivariate receptor model.

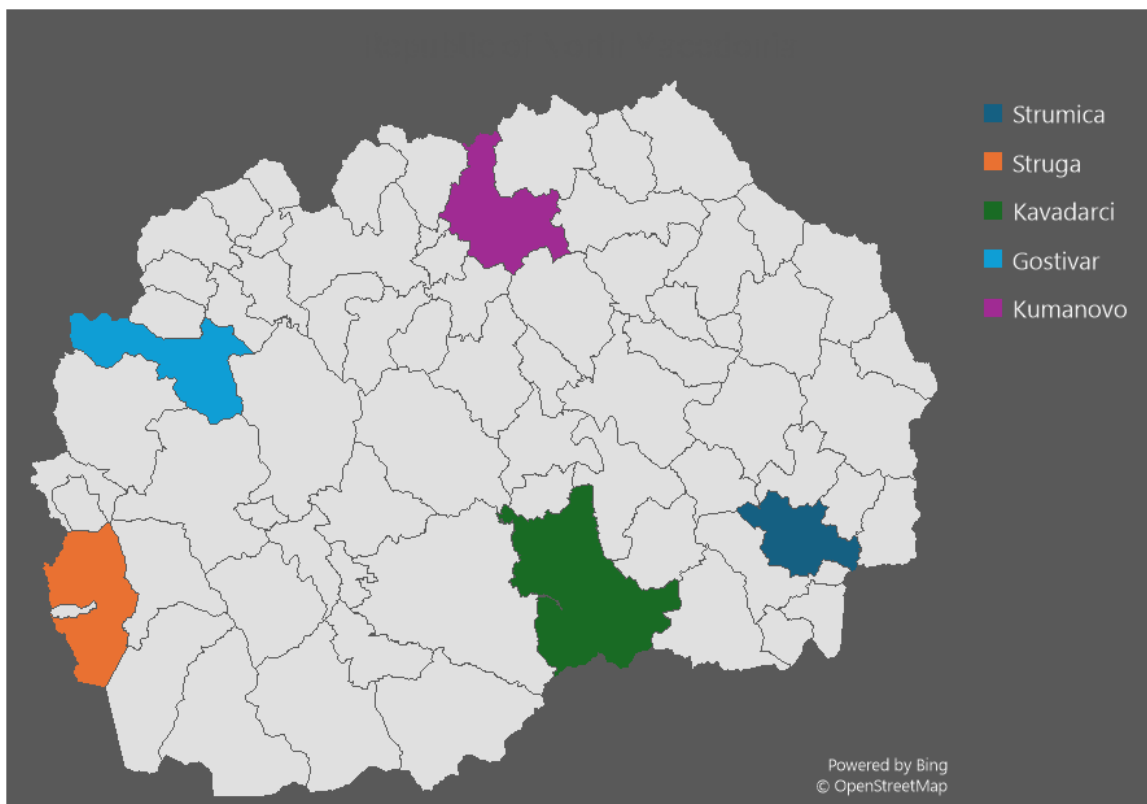


Figure 1. Map of municipalities included in this study

The project also included an indoor air quality study for ten selected public buildings—kindergartens and schools—across the urban areas of five pilot municipalities. The study aimed to assess the current air quality and develop strategies for creating a healthier indoor environment in these facilities.

This research represents one of the first efforts to provide quantitative information on the contributions of various pollution sources to ambient PM2.5 levels in urban centers outside the capital city's urban area. Consequently, the research produced a unique data set that could be used to improve air quality by addressing strategies for mitigating air pollution and implementing effective air protection measures.

2. Background information's

2.1. Kavadarci urban area

The Municipality of Kavadarci is located in the southern portion of North Macedonia and is part of the Vardar Statistical Region. The municipality shares boundaries with the Municipality of Prilep to the west, Chashka and Rosoman to the north, Negotino to the northeast, Demir Kapija and Gevgelija to the east, and Greece to the south. Kavadarci Municipality stretches from Povardarie to Vitachevo, bordered by the Crna Reka and Vardar rivers.

The Tikvesh valley spans 1132 km² and includes the Municipality of Kavadarci, two suburban districts (Glisic and Vatasha), as well as various villages.

According to the 2021 Census, Kavadarci had a total population of 35733, with 12375 households and 14917 houses and apartments.

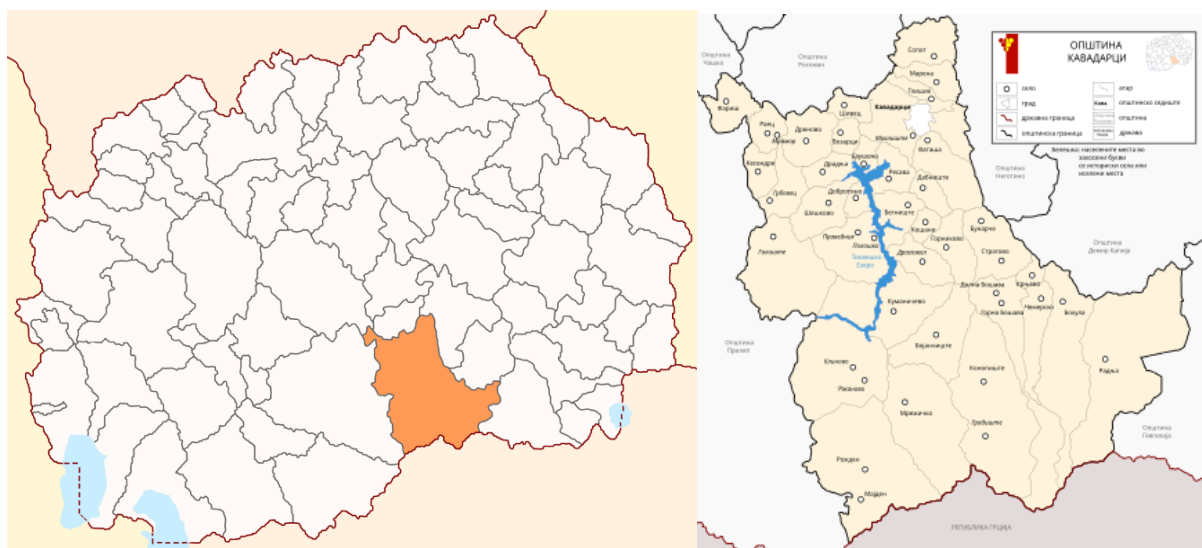


Figure 2. Location of Municipality of Kavadarci [1]

The Municipality of Kavadarci is situated at an elevation of approximately 230 to 270 m above sea level, with an average elevation of 250 m. The municipality spans a range of altitudes, from 200 m in the lowland areas to 2165 m at the peak of Zelen breg on Kozuv mountain.

The Municipality of Kavadarci encompasses the region of middle Povardarie and a section of Crnorechie, stretching from the Tikvesh dam to the confluence of the Vardar river, reaching up to the Vitachevo plateau and including a substantial portion of the Tikvesh valley.

The southern and southwestern regions of the municipality feature high and medium mountains, namely Kozuv and Visheshnica. These mountains transition to the north into a lower, hilly landscape characterized by the Vitachevo plateau and Ljubash hill. The Tikvesh valley's bottom

is distinguished as a unique relief unit characterized by its low-lying terrain. The hydrography of the area includes multiple rivers and two water reservoirs.

Significant rivers include Luda Mara (Velika, Vatashka Reka, Bunarska reka, Kurijska reka), which flows through the town of Kavadarci, along with Crna Reka, Raec, Boshavica, and Doshnica. All these rivers converge into the Vardar River and are part of the Aegean basin. There are two artificial water reservoirs located near Kavadarci. Lake Tikvesh is the largest artificial reservoir in Macedonia by surface area, alongside the smaller Gradot lake located in the upper reaches of the Luda Mara river, formed after the catastrophic landslide on Gradot hill in 1958.

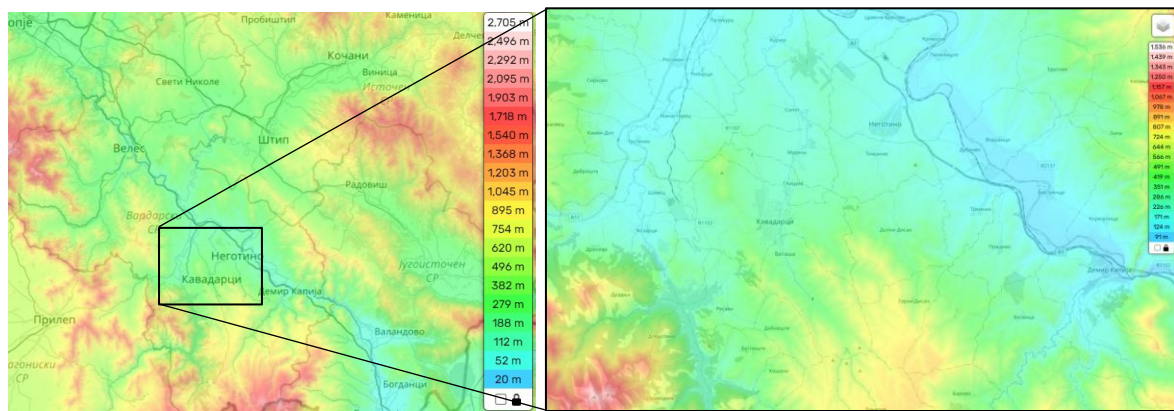


Figure 3. Kavadarci topography map [2]

2.2. Climate

The climatic characteristics of the municipality of Kavadarci are characterized by a modified Mediterranean climate, which is influenced by the Mediterranean climate that permeates the Vardar Valley from south to north, in addition to the moderately continental climatic characteristics of the area. The mountain climate is prevalent in the upper elevations of the Kavadarci municipality. Kavadarci is distinguished by its hot summers and snowy winters, as well as the frequent incidence of early autumn and late spring frosts. The average annual air temperature in the municipality of Kavadarci is 14.2 °C. January is the coldest month in Kavadarci, with an average monthly air temperature of 1.5 °C. July and August are the warmest months, with an average monthly air temperature of 26.5 and 26.6 °C, respectively [3].

The average number of days with temperatures exceeding 30 °C is 68, while the average number of days with temperatures at or below zero is 65. In the municipality of Kavadarci, the autumn months are warmer than the spring months as a result of the Mediterranean climate [1].

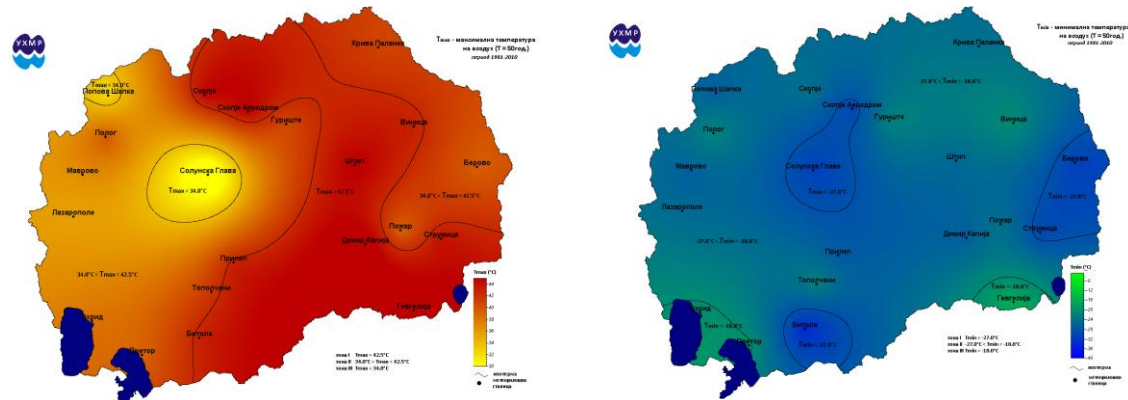


Figure 4. Maximum and minimum temperature maps for North Macedonia with probability of occurrence of 0,002% (Source: Climate maps, UHMR, 2020)

The municipality of Kavadarci receives approximately 466 mm of precipitation annually. July experiences the least precipitation, with an average of 20 millimetres, while December experiences the most precipitation, with an average of 56 millimetres. July and August are the months with the lowest precipitation during the summer, which is the driest period of the year. The average monthly precipitation is 20 mm [3]. The municipality of Kavadarci experiences an average air humidity of 60 %.

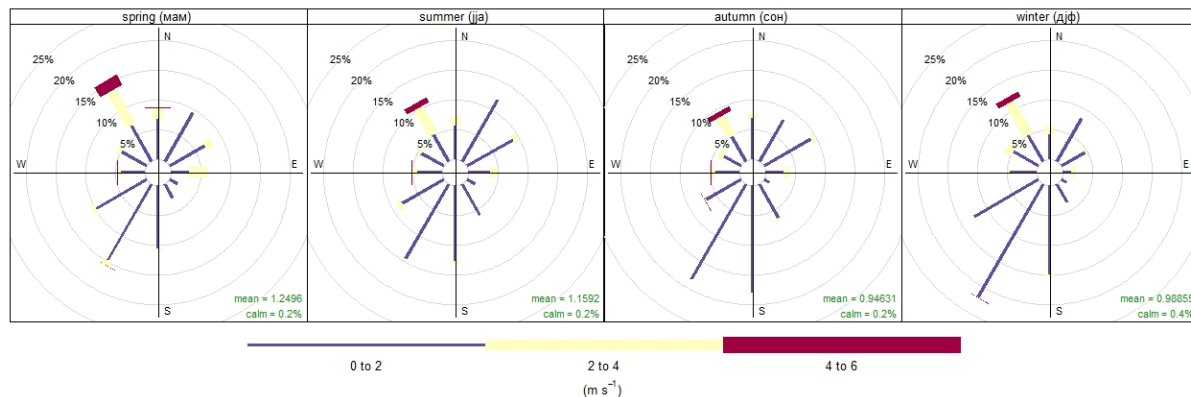


Figure 5. Seasonal wind roses during the monitoring period (March 2023 to February 2024, AMBICON Lab).

The wind roses indicate the majority of winds across all seasons originate from the southwest and south, exhibiting low to moderate speeds, with frequencies ranging from 20 to 25 %. Stronger winds are less common, occurring 10 to 15 % of the time depending on the season, and typically come from the northwest.

The annual insolation duration for Sredno Povardarie is 2230 hours, peaking in July and August. The average consists of 118 clear days, 153 cloudy days, and 94 overcast days [1].

2.3. Transportation and energy infrastructure

The municipality of Kavadarci is strategically positioned to facilitate a rational and efficient connection between the northern and southern regions of the Republic of Macedonia, as well as connecting the eastern areas with Ohrid and Prespa.

The Municipality is connected in the north-south direction via the E-75 corridor, which includes both the highway and the Skopje-Gevgelija railway. These are located 14 km from the city of Kavadarci, accessible through the regional road routes Kavadarci-Negotino and Kavadarci-Rosoman-Gradsko. Kavadarci is linked in the east-west direction by the Gradsko-Prilep-Bitola regional road, located 11 km from the city centre.

In comparison to 2021, when a record high of 11101 vehicles were registered, there were 7314 vehicles registered in Kavadarci in 2022. The figure presents the count of various vehicle types registered in Kavadarci from 2020 to 2022, along with the classification of the vehicle fleet based on the types of fuels utilised [4].

As of January 2023, public transport in Kavadarci is managed by a public company that operates a fleet consisting of 14 vehicles, including buses and vans, as well as one tourist train [5].

In the Kavadarci region, all of the electric power utilised is supplied by the national power network. KEC Kavadarci covers the municipalities: Kavadarci, Negotino, Rosoman and Demir Kapija. It is a relatively large area that is powered by TS 110/35/20/10 kV and TS 35/10 kV. In urban areas such as the city of Kavadarci, the network is mainly cable, while the rest of the outlets are mostly aerial. Renewable sources are represented in this area, mostly small hydroelectric power plants and photovoltaic power plants. The Tikvesh hydroelectric plant is located on the Crna Reka, about 27 km upstream from its confluence with the Vardar River near Kavadarci. This hydro

system has a dual purpose, it is used for the production of electricity and for the irrigation of Tikveshko Pole, one of the hottest and driest regions in North Macedonia.

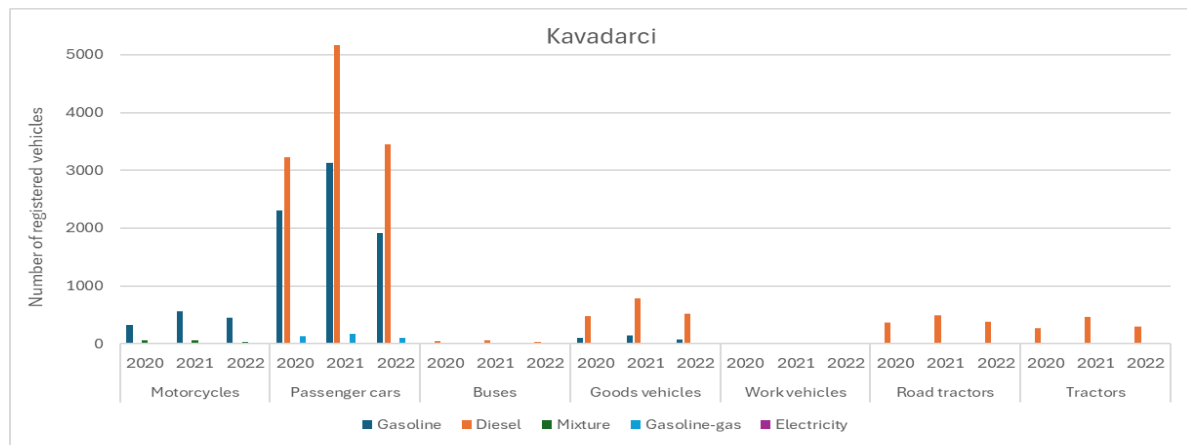


Figure 6. Number of registered vehicles in Kavadarci classified according to the type and fuel used

The largest energy production facility is the Tikvesh hydropower plant, situated at the base of a stone-embankment dam measuring 113.5 m in height, which creates a reservoir with a total volume of 479,000,000 m³ of water. The Tikvesh hydroelectric plant was engineered and constructed with a capacity of 113 MW and an annual output of 144 GWh.

While the Kavadarci region does not have thermal power plants that generate combustion emissions, there is a medium-sized facility, TEC Negotino, powered by residual oil, located approximately 13 km to the east. This plant functions as a reserve system, operating only on a temporary basis and for limited durations.

2.4. Industry and service providers

In the municipality of Kavadarci, only 14 % of the total active business entities are producing businesses, predominantly from the processing industry. There are a few major industrial facilities in Kavadarci Municipality, that are covered by A and B integrated pollution prevention permits. These include the region's largest nickel smelting plant (Euronickel Industry), plants that produce pre-mixed concrete (Energo Maksystem) and asphalt (Diamond Invest), waste treatment facility (Eco Energy System), a meat slaughtering and processing facility (Serta Company), and one of the region's largest wineries (Tikvesh Winery).

Nonetheless, the majority of the plants are situated well beyond the Kavadarci urban area (see Figure 7), with the exception of the winery and meat processing facility, which possess only limited emission potential. Furthermore, owing to energy difficulties in recent years, the primary source of emissions, the nickel smelting plant, has functioned at reduced capacity and was temporarily halted throughout the project's implementation phase.



Figure 7. Sites with industrial infrastructure with IPPC (A and B category) permits [1]

Service providers that operate small or medium combustion plants primarily for heating purposes can also significantly affect urban air quality, as many utilize outdated units fuelled by fuel or residual oil, and in some instances, solid fuels such as lignite or wood. Nine schools, five kindergartens, and a hospital complex are all located inside the boundaries of the urban area (see Figure 8).

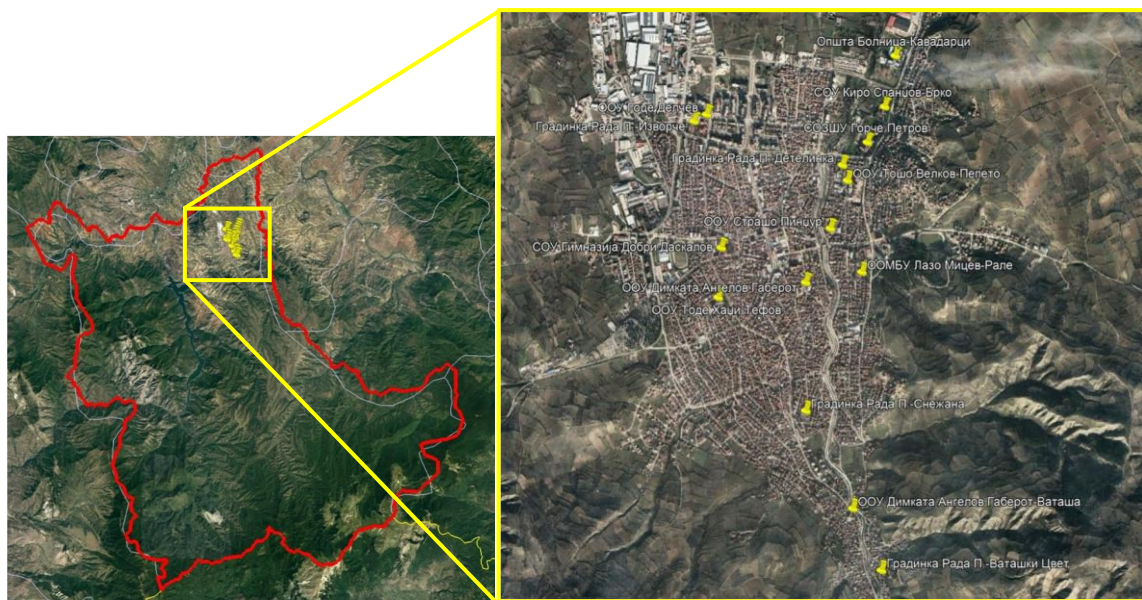


Figure 8. Service providers within Kavadarci urban area [1]

2.5. Historical data on ambient air quality

The last assessment of ambient air quality was conducted as a part of the air quality improvement plan for Kavadarci Municipality [1], utilizing data sourced from the State Monitoring Network covering the years 2017 to 2021.

Data from the Kavadarci monitoring station show that SO₂ average annual concentrations ranged from 1.27 to 2.41 µg/m³, significantly lower than the allowed level of 20 µg/m³ for ecosystem protection, and no reported exceedances of the hourly and daily SO₂ limits for human health protection.

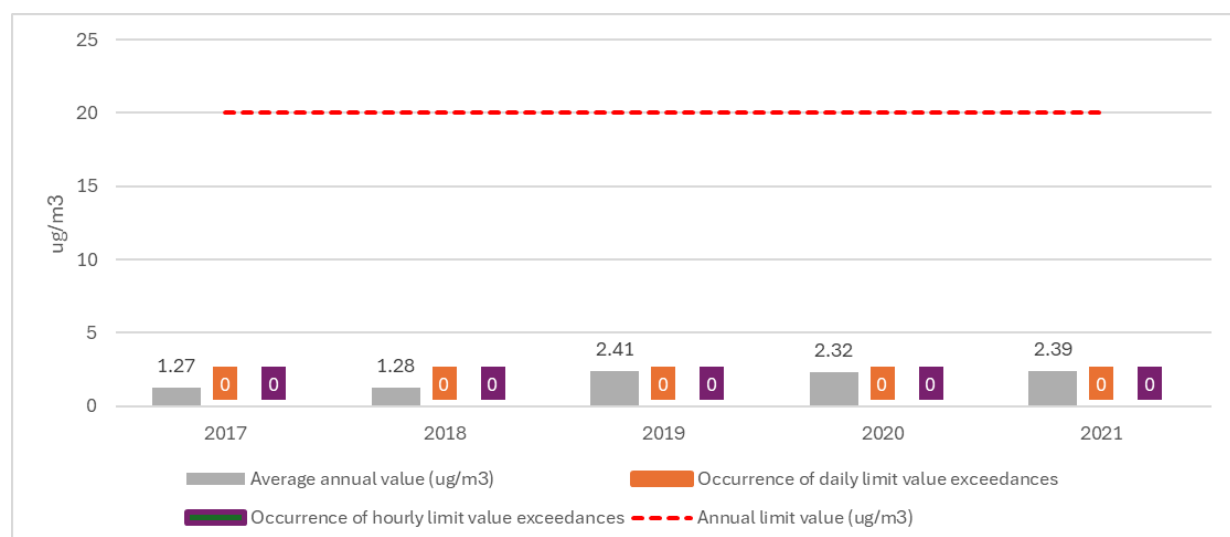


Figure 9. Average annual concentration of SO₂ from 2017 to 2021 [1]

Also, the average yearly concentrations of NO_2 range from 21.64 to 26.92 $\mu\text{g}/\text{m}^3$, well below the established annual limit value of 40 $\mu\text{g}/\text{m}^3$. Furthermore, throughout the specified period, the

hourly threshold values established for the protection of human health (set at $200 \mu\text{g}/\text{m}^3$) were not exceeded.

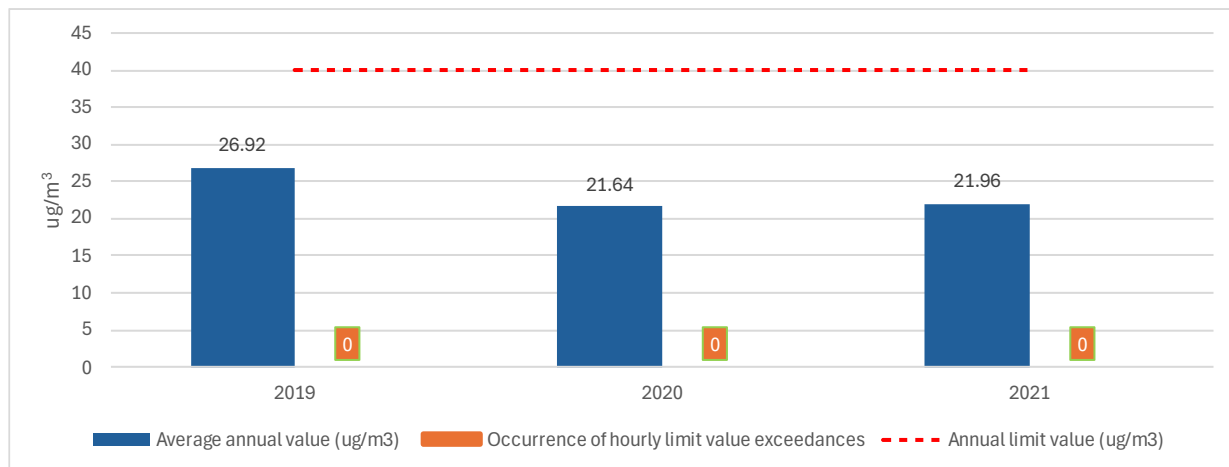


Figure 10. Average annual concentrations of NO_2 from 2019 to 2023 [1]

Carbon monoxide (CO) is similarly regarded as non-critical, as there were no cases of exceeding the health protection target value of $10 \text{ mg}/\text{m}^3$ during the specified time period.

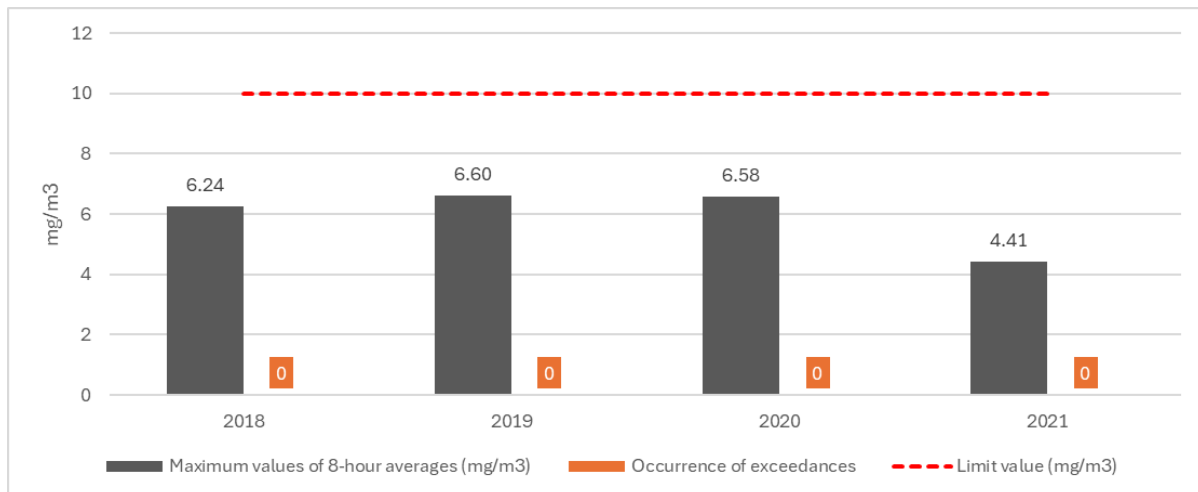


Figure 11. Maximum 8-hour averages of CO from 2018 to 2021 [1]

However, the levels of particulate matter (PM 10) and partially ozone (O_3) consistently surpass the established threshold limits. The ozone data indicate that the human health protection limit of $120 \mu\text{g}/\text{m}^3$ was surpassed in 2018, 2019, and 2021. The highest average ozone values were recorded on July 21, 2018; July 4, 2019; and July 25, 2021. In 2018, the target value for the protection of human health of $120 \mu\text{g}/\text{m}^3$ was surpassed 31 times, 20 exceedances were noted in 2019, and 1 exceedance was recorded in 2021. The observed exceedances ranged from around 21% to only 1% of the limit value, and while not significantly higher, some studies have demonstrated that ozone levels below these requirements can nevertheless result in elevated mortality risks [7]. Lower ozone levels (as low as 40 ppb) have also been shown to have a harmful influence on vegetation and agricultural crops [8, 9].

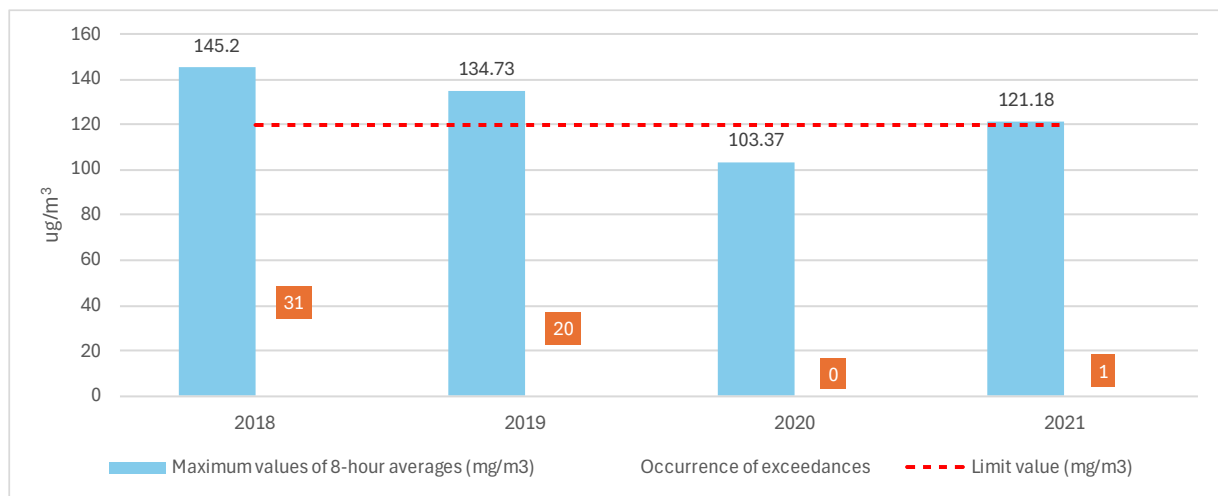


Figure 12. Maximum 8-hour averages of O₃ from 2018 to 2021 [1]

The situation with suspended particulate matter is even worse, since the number of exceedances of the 24-hour limit value and average annual PM10 concentrations in Kavadarci from 2017 to 2021 are consistently higher than the recommended standards.

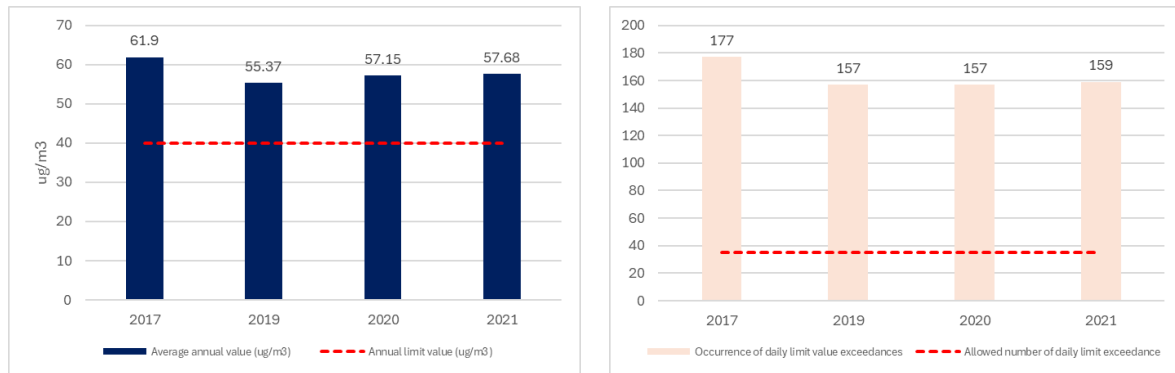


Figure 13. Average annual PM10 concentrations and frequency of exceedances of the 24-hour limit value

As seen above, the total number of 24-hour limit exceedances over a calendar year range from 157 to 177, which is significantly higher than the recommended threshold of 35 days. The annual limit value for human health protection was also dramatically exceeded every year, ranging from 38% in 2018 to 55% in 2017.

For the fine portion of particulate matter (PM 2.5), there is insufficient data to conduct an annual assessment.

3. Major emission sources

Emission data and corresponding source profiles were compiled using several relevant sources, including the Kavadarci Municipality Air Quality Improvement Plan for 2022-2026 [1], as well as the SPECIEUROPE repository [10], which contains chemical profiles of particulate matter obtained from source measurements conducted across Europe.

3.1. Emissions inventory

The emissions inventory has been developed within the Air Quality Improvement Plan [1] by utilizing standardized approaches to estimate air pollutants and greenhouse gas (GHG) emissions across various sectors. Emissions inventories require activity data (e.g., fuel consumption, industrial output) and emission factors that indicate quantity of pollutants released per unit of activity. Data sources commonly include industrial output reports, energy statistics, transportation statistics (vehicle types and usage, fuel consumption), agricultural activities and waste management data. In this particular instance, the primary data sources were official reports from IPPC installations (MOEPP) and the MAKSTAT database (State Statistical Office) [1].

Calculations conducted follow recommended procedures based on the:

- Intergovernmental Panel on Climate Change (IPCC) Guidelines for greenhouse gas emissions.
- European Environment Agency (EEA) EMEP/EEA Air Pollutant Emission Inventory Guidebook – pertaining to air pollutants [11].

Emissions were assessed using the Tier 1 or basic approach, utilizing default emission factors from international sources according to this formula:

$$\text{Emissions} = \text{Activity Data} \times \text{Emission Factor}$$

where:

- Activity Data denotes the quantity of a particular activity (e.g., fuel consumed in tons).
- Emission Factor denotes emissions per unit of activity (e.g., kg of PM 2.5 per ton of fuel combusted).

In accordance with national regulations and guidelines (Nomenclature For Reporting - NFR and Guidelines for Drafting AQIP) [55], this inventory categorizes emissions into the following sectors: industry, transportation, public sector (administration and services), residential sector (households), agriculture (which includes livestock and fertilizer usage), waste management (including emissions from landfills, wastewater treatment, and waste incineration) and natural sources.

The annual emissions of criteria pollutants have been calculated [1] and are detailed in Table 1.

Table 1. Criteria pollutants emissions (in tons per year) for Kavadarci municipality [1]

	Pollutants (t/year)							
	NOx	CO	NMVOC	SOx	NH ₃	TSP	PM10	PM2.5
Industry	382,10	402,04	149,11	1453,12	/	553,63	152,27	64,41
Public facilities	4,76	3,39	1,37	1,40	0,13	0,91	0,89	0,84
Households	8,43	643,61	96,43	2,33	11,23	128,50	122,07	118,86
Traffic	108,26	108,71	28,47	11,72	1,43	14,92	13,00	11,41
Waste	0,64	11,25	26,50	0,02	/	0,94	0,91	0,84
Agriculture	17,29	/	20,19	/	86,16	12,55	3,04	0,89

As illustrated above, industrial activities and household heating are the predominant sources of particulate matter emissions, with industry accounting for 52% of PM10 emissions and household heating comprising 60% of PM2.5 emissions. Considering that the principal industrial emission source, the nickel smelting plant, was temporarily closed throughout the monitoring period, it is reasonable to conclude that the residential sector (household heating) was the predominant emission source during this timeframe.

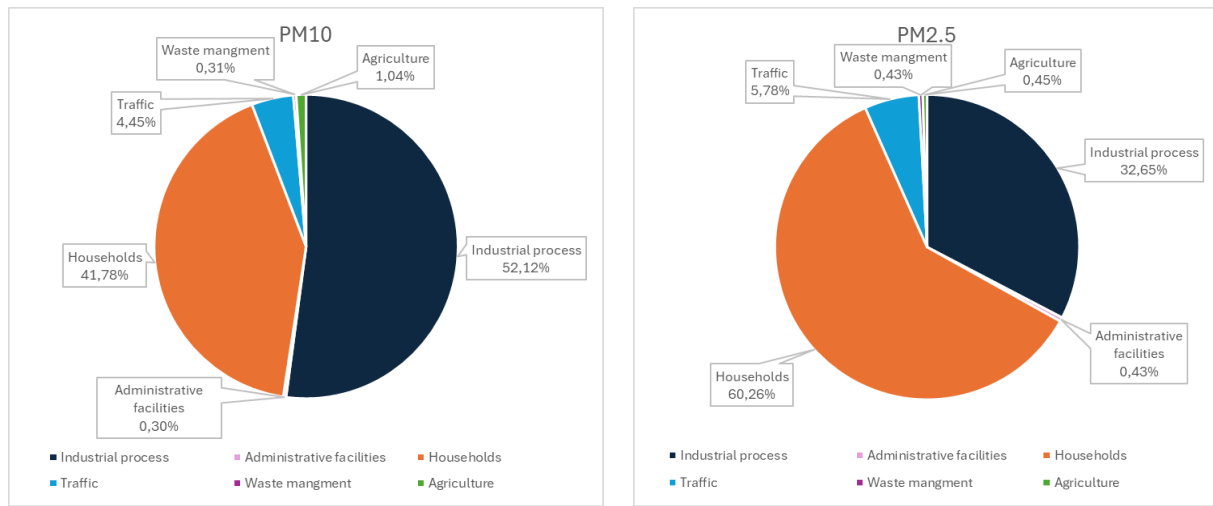


Figure 14. Sectoral contribution to particulate matter emissions [1]

3.2. Source profiles

Chemical profiles of the sources identified in the inventory were obtained using the data published in SPECIEUROPE, a repository of source profiles developed by the JRC in the framework of FAIRMODE project [13]. SPECIEUROPE comprises chemical profiles of particulate matter, both organic and inorganic, derived from measurements of European sources and source apportionment investigations conducted in Europe.

Based on data given in the emission inventories, chemical profiles for following sources are included:

- Woodstove burning
- Open burning of crop residues
- Construction
- Traffic urban + Vehicle Exhaust
- Soil dust + Road dust
- De-icing Salt
- Fuel oil + Residual oil

The chemical profile of the nickel smelting plant has been intentionally omitted, as the plant was non-operational throughout the entire monitoring campaign.

A brief description of the sources, sampling and analytical procedures that were employed, geographical location, elemental composition (relative mass of the elements), and bibliography are provided in the sections that follow.

Woodstove burning profile is based on JRC data, referencing closed fireplace wood combustion in Krakow, Poland. Elemental analysis was performed using particle induced x-ray emission (PIXE), photometric and ion chromatography (IC) methods are used for water soluble ions analysis, thermal optical analysis (TOT) was used for OC and EC analysis, and gas

chromatography-mass spectrometry (GC-MS) for organic compounds. Organic carbon (OC) and elemental carbon (EC) are by far most abundant compounds (89.63 and 6.65 % respectively), followed by K (1.11 %) and Cl (0.43 %). Sulphates (0.87 %) and nitrates (0.25 %) are most abundant ions.

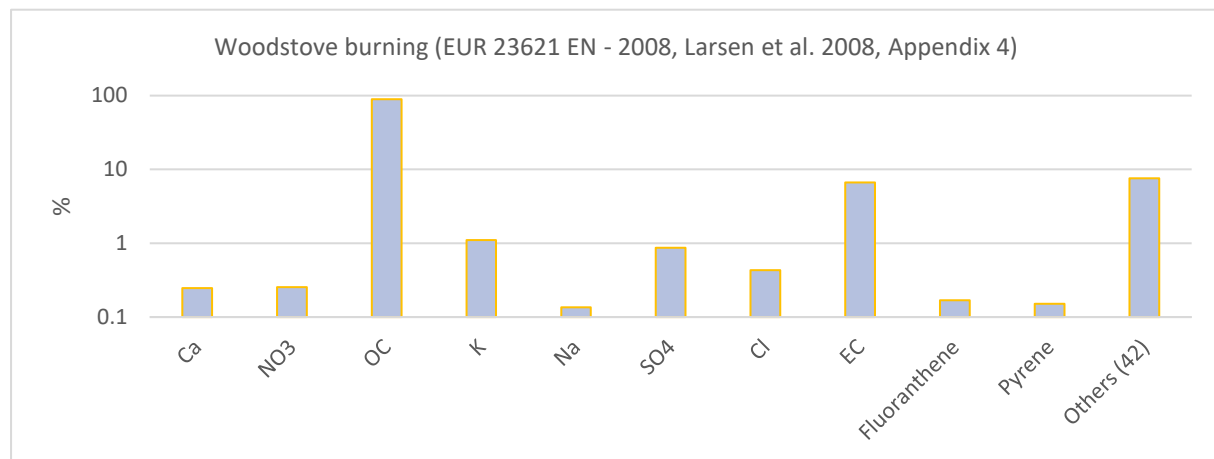


Figure 15. Woodstove burning chemical profile (closed fireplace)

Open burning of crop residues, or agricultural fields burning profile is based on direct on filter samples from Thessaloniki area in Northern Greece. Samples were analysed using energy dispersive X-ray fluorescence (ED-XRF) for elemental composition and ion chromatography (IC) for water soluble ions analysis. Bromine is most abundant element (9.43 %), followed by EC (9.0%) and Co (9.0 %). Other metals including V (8.133 %), Ti (4.83 %) and As (1.1 %) also have significant concentrations. Sulphates (8.13 %) are by far most abundant ion.

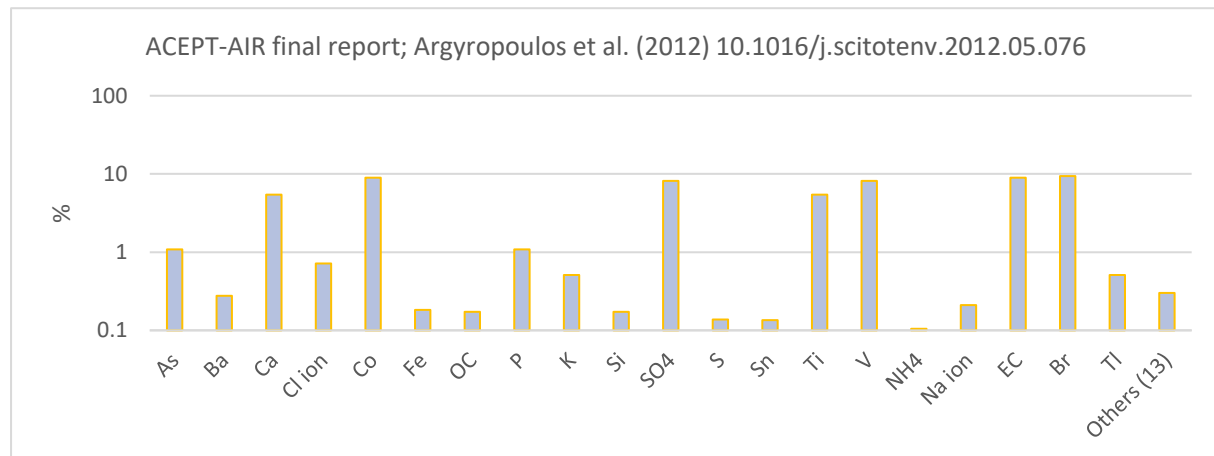


Figure 16. Open burning of crop residues chemical profile

Construction activities source profile is based on data obtained from Milan, Italy. Specific information's about sampling and analytical procedures used, were not provided. Calcium is most abundant element (19.85 %), closely followed by OC (17.9 %) and Si (12.55 %). Other metals including Ni (7.66 %), Al (3.78 %), Fe (1.91 %) and K (1.71 %) also have significant concentrations. Sulphates (9.14 %) and ammonium (1.96 %) are most abundant ions.

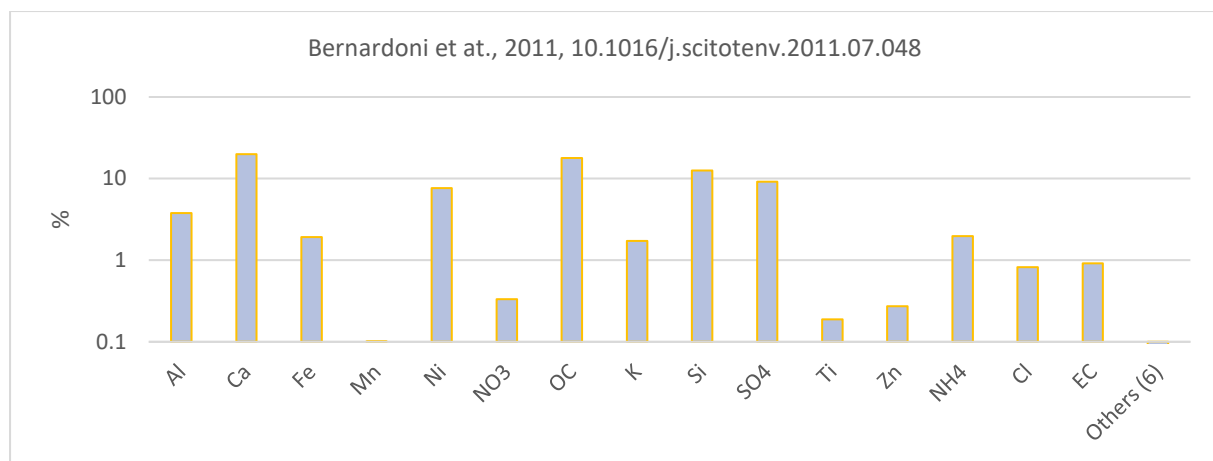


Figure 17. Construction activities chemical profile

Traffic source profile include two separate profiles, exhaust diesel and gasoline and urban traffic profile, based on data from PMF exercises in Valtellina, Po Valley, and Genoa Corso, Firenze in Italy. Specific information's about sampling and analytical procedures used, were not provided. OC and EC are most abundant compounds in both profiles, OC (53.59 and 35.1 %) and EC (30.46 and 23.04 %) respectively. Some metals including Fe (13.56 and 2.34 %), Cu (1.1 %) and Si (0.89%) in mixed exhaust and Ca (1.89 %) in urban traffic mix, also have significant concentrations. Sulphates (5.05 %) are by far most abundant ion in mixed exhaust, while ammonium (1.68 %) and nitrates (1.51 %) are most abundant ions in urban traffic mix.

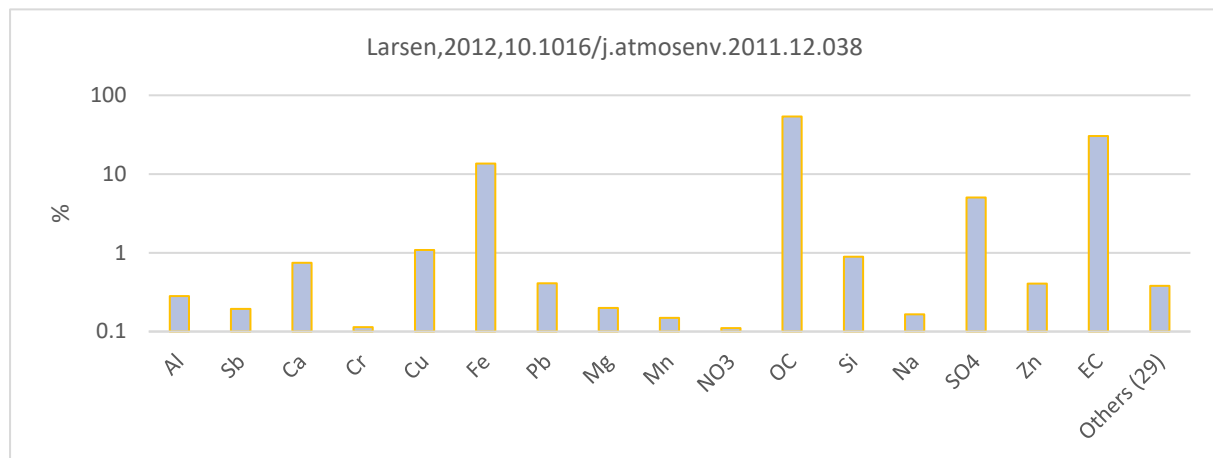


Figure 18. Exhaust diesel and gasoline chemical profile

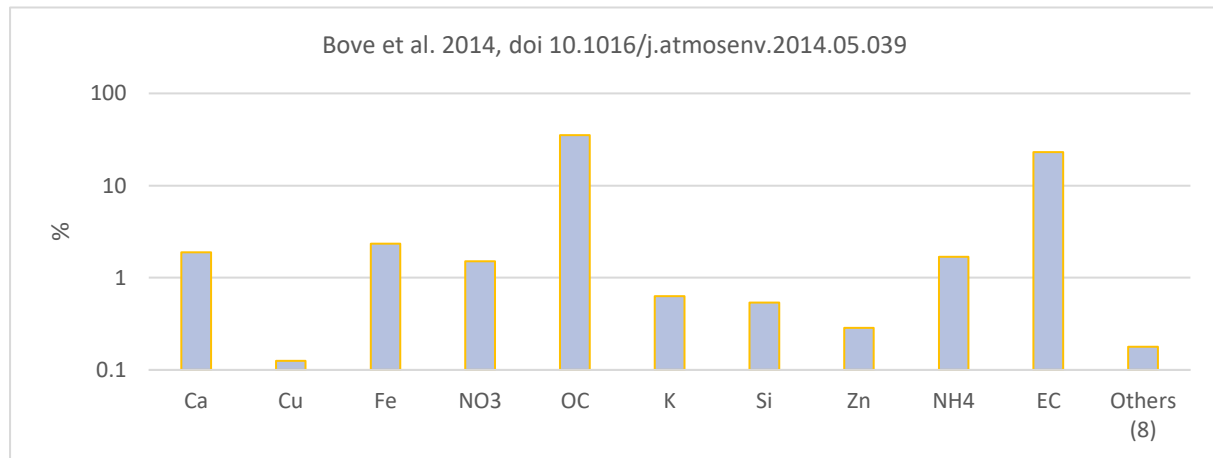


Figure 19. Urban traffic chemical profile

Road dust is another profile associated with traffic emissions. The profile selected is based on data from PMF exercises in Valtellina, Po Valley in Italy. Description of sampling and analytical procedures used, was not included. Silica is most abundant elements (15.63 %), followed from OC (7.25 %), Al (7.07 %), Fe (4.19 %), Ca (2.41 %), Mg (1.37 %) and K (1.43 %). No significant concentrations of water-soluble ions were reported.

Soil dust profile is based on grab dust samples collected from the fabric filter from Thessaloniki area in Northern Greece. Samples were dried and resuspended in a puff of clean air, then sampled with PM10 inlet with LVS, and analysed using energy dispersive X-ray fluorescence (ED-XRF) for elemental composition and ion chromatography (IC) for water soluble ions analysis. Silica is most abundant element (20.9 %), followed by Al (5.65 %), Fe (4.36 %), Ca (3.20 %), Mg (1.56 %), K (1.37%) and Ti (0.41 %). No significant concentrations of water-soluble ions were reported.

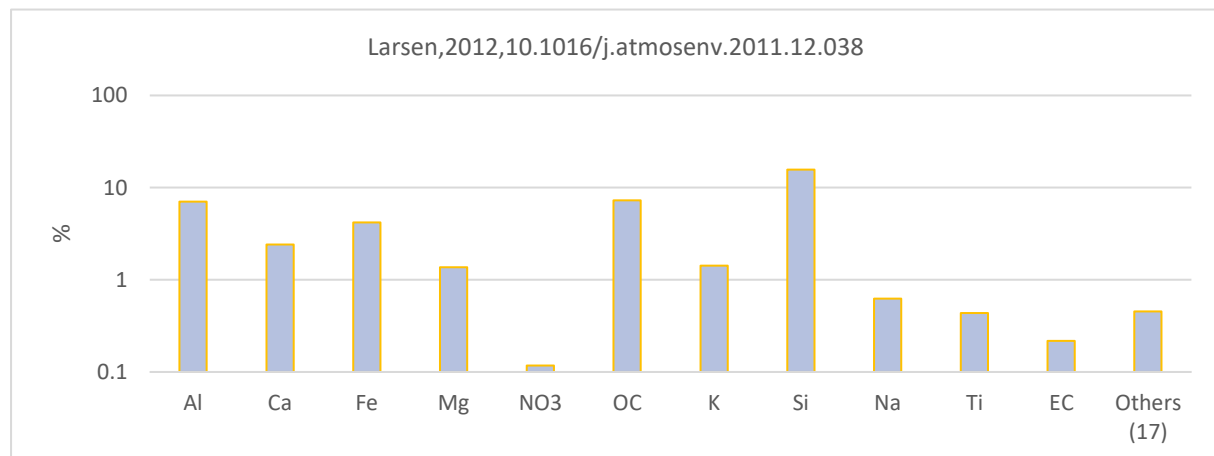


Figure 20. Road dust chemical profile

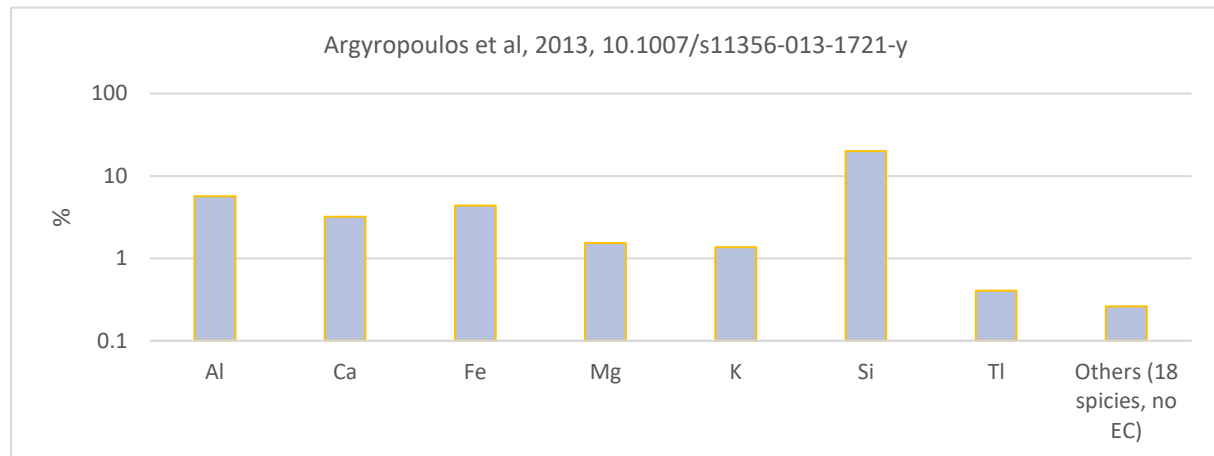


Figure 21. Soil dust chemical profile

Fuel and residual oils burning includes emissions from a wide range of sources, the majority of which are larger buildings heating systems (schools, hospitals, and other public institutions), industrial combustion emissions and to some extent older diesel-powered vehicles emissions.

Residual oil chemical profile is based on data from PMF exercise in Genoa Corso, Firenze in Italy. Samples were analysed using energy dispersive X-ray fluorescence (ED-XRF) for elemental composition, ion chromatography (IC) for water soluble ions analysis, and thermal optical analysis (TOT) for OC\EC analysis. Elemental carbon is by far most abundant compound (31.3%), followed by sulphates and ammonium ions (23 and 5.75 % respectively). As of metals, iron and

vanadium exhibit highest concentrations (0.98 and 0.76 % respectively), followed by Ni (0.28 %), K (0.128 %) and Ca (0.10 %).

Fuel oil chemical profile is based on JRC data on small (<5MW) fuel oil boilers emission in Krakow, Poland. Specific information's about sampling and analytical procedures used, were not provided. Organic carbon is most abundant compound (25.3 %), followed by nitrates (18.53 %) and sulphates (13.78 %). Other elements include Ca (1.2 %), Cl (1.16 %), Mg (0.57 %), Al (0.42 %), V (0.16 %) and Ni (0.14 %).

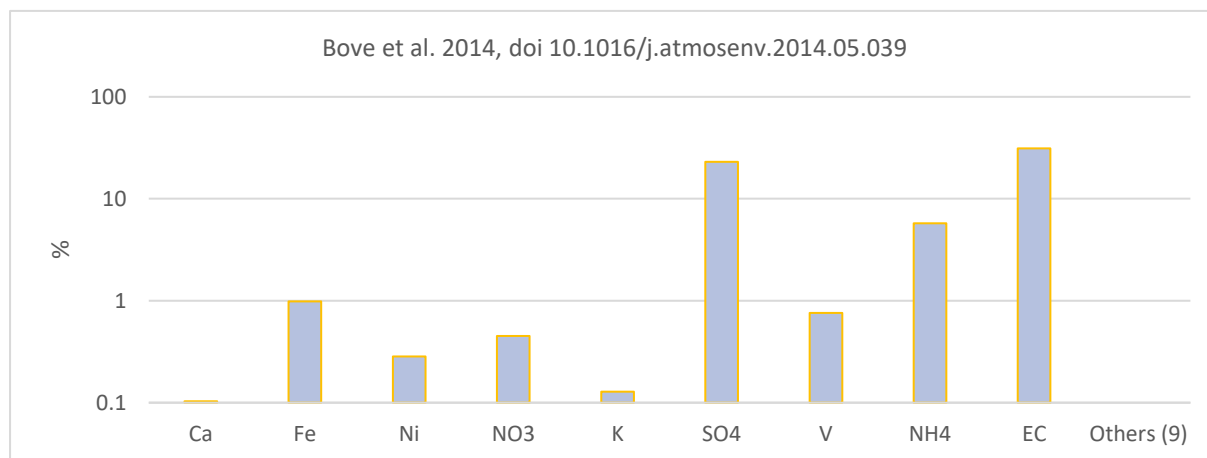


Figure 22. Residual oil chemical profile

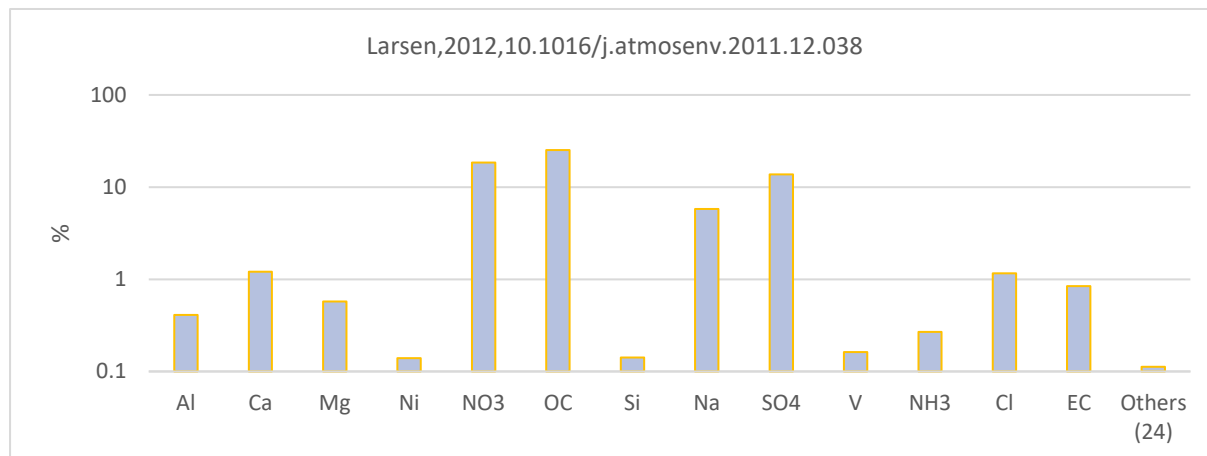


Figure 23. Fuel oil chemical profile

The source profiles outlined above were utilized to assign source categories to factors generated during positive matrix factorization. This procedure was supported with quantitative and descriptive comparison of the factor chemical profiles with those measured at the source and profiles from previous source apportionment studies in the literature, as given above.

4. Particulate matter sampling and analysis

Given the goals of the SA study, the available data, and the project document needs, we chose and set up one specific receptor/sampling point in the urban areas of Kavadarci.

The sampling point in Kavadarci, integrated with the state monitoring network (our code MP1-AQP), is situated at the junction of two major roads on the outskirts of the city. This location experiences a significant volume of traffic.

Kavadarci is situated in a region known for wine production, and the Tikvesh winery, which is the closest source of emissions, is located 500 meters from the station. The FENI industry is the primary source of particle pollution in the area. The smelting factory is situated 5 kilometers to the west of the Kavadarci station. However, it is positioned on the opposite side of the hills, which mitigates the spread of pollutants towards the urban area, and the plant was temporarily halted throughout the project's implementation phase.



Figure 24. Monitoring location in Kavadarci urban area

The sampling program at this site began on March 8, 2023. Every other day, we collected a 24-hour sample. A total of 182 samples were collected in Kavadarci from March 8, 2023, to April 27, 2024.

All quality assurance and quality control steps for preparing, handling, and storing the filters were done following the Standard Operating Procedure of the UGD AMBICON Lab, which is certified to ISO 17025 for environmental sampling and testing.

4.1. Sampling and determination of mass concentration of ambient particulate matter (PM2.5)

Sampling process was performed fully in line with the requirements of standard gravimetric measurement method for determination of the PM10/PM2,5 mass concentration of suspended

particulate matter (EN 12341:2014). Sampling was performed on 47 mm PTFE filters (Advantec depth filter PF 020 and PF 040), according to Standard Operating Procedure of the UGD AMBICON Lab, an ISO 17025 accredited for environment and samples from the environment testing (<https://iarm.gov.mk/en/2021/07/01/lt-052-university-goce-delcev-shtip/>).

Sampling procedure

The sampling site was equipped with low/medium volume sequential sampling system (PNS 18T-DM-6.1, Comde Derenda, Germany), certified as a reference device for PM2.5 sampling according to EN 12341:2014.

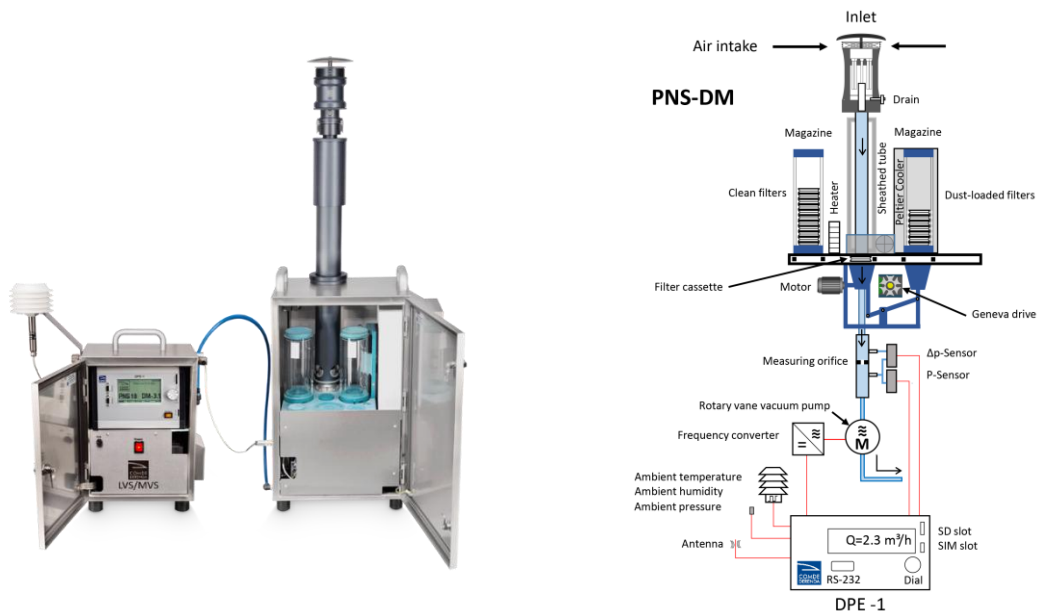


Figure 25. Sequential sampling system PNS 18T-DM 6.1

Sequential sampling systems provide fully automatic sampling according to pre-set parameters. Session from 14 to 16 days were set for each site. Each initial magazine was loaded in the AMBICON Lab premises with 16 to 18 filters, of which top one was not used for sampling, but as a protection in order to collect possible passive particle deposits. Additional one was transferred to the storage magazine without exposure and used as a field blank.

All monitoring data were electronically recorded, including sample ID, pump runtime, time of measurement, motor speed, actual flow, normalized flow, volume sampled-actual, volume sampled-normalized, filter pressure, ambient air pressure, outdoor temp, filter temp, chamber temp and relative humidity. During each filter magazine change operation or at a period of 14 to 16 days, several quality assurance and control procedures were performed, including:

- sampling head cleaning,
- reading accuracy check for all sensors, and
- leak tightness test.

Sampling head, including inside of the tubular casing, the intake side of the multijet unit, the impaction plate and the jet tubes will be cleaned with alcohol and wiped with dry cloth. Impaction plate will be greased with silicone spray lubricant. The insect screen will be checked for obstructions and cleaned if necessary. Notes about cleaning and visual inspection were recorded in lab sampling logbook.

Reading accuracy of all sensors was checked through a short sampling test cycle, all the while, readings of the sensors was compared against external calibrated standards, including:

- test of flow rate set, against the reading of calibrated external flow meter (with certificate issued from ISO 17025 calibration lab),
- test of system temperature, humidity and ambient pressure readings, against calibrated external ambient Temp and RH meter (with certificate issued from ISO 17025 calibration lab),

Data about readings from all sensors were recorded in separate form of lab sampling logbook.

Leak tightness test of the system was performed through a low-pressure method, fully according to section 5.1.7.2 of the EN 12431:2014. The system has integrated leak test procedure, where pump is run, with closed calibration adapter until 400 hPa under-pressure in chamber is reached. The pump is switched off, and after 5 minutes pressure is read from the screen. If the value of under-pressure in the chamber is above 210 hPa, the system has passed the run test. According to above norm requirements, the test was repeated 3 times (total 3 runs). Data from the test runs were recorded in separate sheet of lab sampling logbook.

Filters handling and weighing

Prior to sampling, all filters were uniquely identified and conditioned at 19 °C to 21 °C and 45 to 50 % RH in climate chamber (ICH 110, Memmert, Germany) for ≥ 48 h, and weighted twice with at least 12 hours reconditioning period, to confirm mass stabilization (qualified difference < 40 μg). For each batch, two (2) blank filters are left to serve as a weighing room blanks.



Figure 26. Weighing room- AMBICON UGD Lab

After each sampling session, storage and initial magazine were removed from the housing. Protective reference filter was removed from the magazine and discarded, while empty magazine was fixed as new storage magazine. As soon as removed from the housing, storage magazine was sealed with cap and parafilm and stored in transportation “cool box”. Sampled filters after exposure were returned to the weighing room and conditioned in a controlled temperature and humidity chamber for more than 48 hours and weighted. After additional conditioning period of

minimum 24 hours, filters were re-weighted and accepted as stabilized if difference between results is $\leq 60 \mu\text{g}$. Same conditions was applied for filed blanks.

Weighing was performed with electronically controlled micro balance Radwag MYA5.3Y.F (resolution $d = 1 \mu\text{g}$), installed within controlled temperature and humidity room and completed with antistatic ionizer. Weighing data set and room conditions were electronically recorded.

Ongoing quality control were performed fully in line with the requirements of standard gravimetric measurement method for determination of the PM10/PM2,5 mass concentration of suspended particulate matter (EN 12341:2014), according to standard operating procedure of UGD AMBICON Lab, an ISO 17025 accredited for environment and samples from the environment testing areas.

Measurement uncertainties were calculated following GUM concept (JCGM 100) and included all individual uncertainty sources.

Mass concentration of ambient particulate matter was calculated as the difference in mass between the sampled and unsampled filter, divided by the sampled volume of air, determined as the flow rate multiplied by the sampling time. Measurement results are expressed as $\mu\text{g}/\text{m}^3$, where the volume of air is that at the ambient conditions near the inlet during sampling.

Data collected and comments are included in each filter testing results, given as supplementary material to this report (A – 1 Mass concentration of ambient particulate matter).

4.2. Chemical speciation

The elemental analysis of collected atmospheric aerosols (PM2.5) is the initial step in determining their sources and environmental impact. It can be accomplished by several methods. Certain analytical procedures are prohibitively expensive, others are labor-intensive, and some approaches result in sample destruction. This study utilized energy dispersive X-ray fluorescence (ED-XRF) for elemental composition analysis, optical transmissometer for measuring elemental carbon content, and spectrophotometry for the detection of water-soluble ions.

Elemental analysis using energy dispersive X-ray fluorescence spectrometry

The elemental analysis of PM2.5 of aerosols was conducted using energy dispersive X-ray fluorescence spectrometer NEX CG produced by Rigaku. The secondary targets of the NEX CG substantially improve detection limits for elements in highly scattering matrices including water, hydrocarbons, and biological materials, and a unique close-coupled Cartesian Geometry optical kernel significantly increases signal-to-noise. The spectrometer is capable of routine trace element analysis even in filter samples, thanks to the remarkable reduction in background noise and corresponding increase in element peaks [13].

Analyses were carried out in the AMBICON Lab, at Goce Delcev University in Stip, North Macedonia, according to the EPA/625/R-96/010a Compendium of Methods, Method IO-3.3: determination of metals in ambient particulate matter using x-ray fluorescence (XRF) spectroscopy published by U.S. Environmental Protection Agency.



Figure 27. NEX CG by Rigaku

The calibration curve on the NEX CG was generated utilizing certified standard reference materials from UC Davis, Air Quality Research Center, University of California (USA), alongside SRM2783 from the National Institute of Standards and Technology (USA) and select single element certified reference materials from Micromatter (Canada). The calibration primarily utilized three multi-element reference materials, encompassing 28 components, which simulated atmospheric PM composition and covered a range from UC Davis. In addition to these three loaded filters, one UC Davis blank filter was also utilized.

Alongside continuous quality control and weekly monitoring of the certified reference filters (Table 2), we also ensure quality through inter-laboratory comparisons (Table 3).

Table 2. Quality control results of EDXRF NEX CG by Rigaku

Element	Certified reference concentration (ng/cm ²)	Average	Standard deviation	Coefficient of variation (%)	Recovery (%)
Na	178.43	149.76	31.18	20.82	100.0
Mg	89.84	89.11	3.88	4.36	100.0
Al	376.00	373.29	11.40	3.05	100.0
Si	1168.57	1159.05	21.19	1.83	100.0
P	9.17	9.09	0.27	2.95	100.0
S	1644.29	1644.29	46.11	2.80	100.0
K	2628.57	2640.00	25.50	0.97	100.0
Ca	3622.86	3623.81	22.91	0.63	100.0
V	8.20	8.17	1.13	13.81	100.0
Cr	81.00	82.80	2.12	2.56	100.0
Mn	24.99	26.66	3.00	11.27	100.0
Fe	733.14	728.86	14.74	2.02	100.0
Co	37.43	41.63	5.24	12.59	100.0
Ni	60.00	64.76	5.03	7.76	100.0
Cu	26.50	28.15	5.70	20.23	100.0
Zn	103.30	105.21	5.57	5.30	100.0
As	142.17	151.95	25.94	17.07	100.0

Element	Certified reference concentration (ng/cm ²)	Average	Standard deviation	Coefficient of variation (%)	Recovery (%)
Se	88.00	89.06	5.35	6.01	100.0
Zr	20.50	21.17	1.04	4.92	100.0
Mo	18.79	18.80	0.53	2.81	100.0
Cd	440.71	482.71	48.49	10.05	100.0
Ba	75.29	74.83	4.54	6.07	100.0
Pb	210.00	195.13	15.68	8.04	100.0

The inter-laboratory comparison was conducted directly between AMBICON Lab and the Institute of Nuclear & Radiological Sciences and Technology, Energy & Safety (INRASTES), affiliated with the National Centre for Scientific Research Demokritos in Greece. A comprehensive comparison was performed using 21 PTFE filters with different loadings, comprising 20 samples and 1 blank. The findings from the calculated Zeta-score have been considered acceptable, as presented in Table 3.

Table 3. Zeta-score results of EDXRF inter-laboratory comparison

Element	Zeta Score	Element	Zeta Score	Comments/Notes
Na	1.68	Ni	0.34	Explanation of Zeta-score values: $ z \leq 2.0$ the result is considered acceptable
Mg	1.21	Cu	2.31	$2.0 < z < 3.0$ indicate a warning signal
Al	1.69	Zn	0.80	$ z \geq 3.0$ results are considered unacceptable
Si	1.34	S	0.41	
Mn	1.04	K	0,67	
Fe	0.80	Ca	1.34	
Cr	0.39	Ba	2.49	
Pb	1.09			

Analysis of water-soluble ions

Water-soluble ions were extracted from the aerosol filters using sonication and shaking as recommended in the in-house developed Standard Operating Procedure for PM2.5 Cation Analysis [14]. The filters were cut in half using ceramic scissors and the mass of the filters was determined using electronically controlled micro balance with resolution of 1 µg. Half of the filter is placed in plastic centrifuge tubes filled with 25 mL ultra-pure water ($> 18\text{M}\Omega\text{-cm}$) and sonicated on room temperature in the ultrasonic bath (GT Sonic Pro, UK) for 60 minutes. Ice was added in the ultrasonic bath to keep the temperature below 27°C. After the sonication, the centrifuge tubes were shaken for 9 hours at 640 rpm using IKA KS 130 orbital shaker. After the procedure is completed, and in order to provide time for sample stabilization, the samples were stored in refrigerator overnight.

Water-soluble ions, including sulphates (SO₄²⁻), nitrates (NO₃⁻) and ammonium (NH₄⁺) have been measured photometrically using the Spectroquant® Prove 600 spectrophotometer by Merck.

Ammonium ions were analyzed using 1.14752.0001 Spectroquant® cell test analogous to EPA 350.1, ISO 7150-1 and DIN 38406-5 methods and detection limit of 0.015 mg/l NH₄⁺. Quality control was provided using Certipur - certified reference solution of NH₄Cl in H₂O (1000 mg/l NH₄⁺) traceable to NIST.

The sulphate ions were analyzed using 1.01812.0001 Spectroquant® cell test analogous to EPA 375.4, APHA 4500-SO₄²⁻E, and ASTM D516-16 methods and detection limit of 0.5 mg/l SO₄²⁻. Quality control was provided using Certipur - certified reference solution of Na₂SO₄ in H₂O (1000 mg/l SO₄) traceable to NIST.



Figure 28. Spectroquant® Prove 600, Merck

Nitrate ions were analyzed using 1.09713.0001 Spectroquant® cell test analogous to DIN 38405-9in method and detection limit of 0.2 mg/l NO₃⁻. Quality control was provided using Certipur - certified reference solution of NaNO₃ in H₂O (1000 mg/l NO₃⁻) traceable to NIST.

Table 4. Quality control results for water soluble ions standard operating procedure

Ion	Concentration in certified reference solution		Average	Standard deviation	Coefficient of variation (%)	Recovery (%)
	mg/l	Certified reference solution				
NH ₄ ⁺	0,1	NH ₄ Cl in H ₂ O (1000 mg/l NH ₄ ⁺), Certipur	0,10	0,02	19,81	100,0
SO ₄ ²⁻	10	Na ₂ SO ₄ in H ₂ O (1000 mg/l SO ₄), Certipur	10,31	0,70	6,76	100,0
NO ₃ ⁻	10	NaNO ₃ in H ₂ O (1000 mg/l NO ₃ ⁻), Certipur	9,64	0,61	6,33	100,0

Elemental Carbon analysis

Black Carbon or Elemental Carbon was determined using Magee Scientific, SootScan™ Model OT21 Optical Transmissometer with dual wavelength light source (880nm providing the quantitative measurement of Elemental Carbon in PM, and a 370 nm for qualitative assessment of certain aromatic organic compounds), by applying EPA empirical EC relation for Teflon FRM filters.



Figure 29. Magee Scientific, SootScan™ Model OT21 Optical Transmissometer

The reproducibility of the photometric detector is validated using a Neutral Density Optical Kit, which is traceable to NIST and recommended by the manufacturer.

4.3. Observations and results

This sections present observations from the monitoring program conducted in Kavadarci, starting from March 2023 and ending March 2024. Results present daily variations in mass concentrations and chemical composition of PM with respect to various chemical species including carbon fraction (Elemental Carbon), crustal elements (Al, Si, Ca, Ti and Fe), water soluble ions (NH_4^+ , SO_4^{2-} , NO_3^-) and larger group of other elements (Na, Mg, P, S, Cl, K, V, Cr, Mn, Co, Ni, Cu, Zn, As, Se, Br, Rb, Sr, Zr, Mo, Cd, Ba, Pb).

Statistical Evaluation

Descriptive statistics help us summarize, describe, and illustrate the data in a more meaningful fashion, making data interpretation easier. Therefore, we provide a summary of descriptive coefficients for each of the sites included in the monitoring program below.

The descriptive statistical analysis presented includes both categories: measures of central tendency and measures of variability (or variation).

Measures of central tendency are techniques for describing the position of the center of a frequency distribution for a given set of data. Although numerous statistics such as the mode, median, and mean can be used for this purpose, the middle position in this case is represented by the arithmetic mean.

Measures of variability provide a summary of a data set by illustrating the distribution of the observed results. Several statistics to explain this spread are utilized, including minimum, maximum, quartiles, variance, and standard deviation. Descriptive coefficients are combined with tabular and graphical descriptions, along with comments and discussions of the results.

Additionally, a correlation matrix illustrating the relationship between all values in the dataset is provided as a basic tool for summarizing large datasets and identifying and visualizing data relationships.

The correlation matrix table contains the correlation coefficients between each variable based on the Pearson parametric correlation test and is color-coded for correlation values above ± 0.6 . In this case, correlation matrices show how the species are related, pointing out their shared sources, and they are also used for exploratory factor analysis and checking data quality.

Table 5. Statistical evaluation – Kavadarci dataset

	Units	N	Mean	SD	Minimum	Maximum	C.V.	95 th %	5 th %
PM2,5	µg/m ³	182.0	62.2	29.2	14.7	154.8	46.9	120.6	19.3
Na	ng/m ³	182.0	113.0	150.3	5.5	871.3	133.0	461.6	5.5
Mg		182.0	86.5	49.3	0.7	262.9	57.0	195.1	18.0
Al		182.0	365.8	221.8	0.5	1078.6	60.6	914.7	79.7
Si		182.0	1218.8	714.6	5.6	3605.6	58.6	2911.1	297.9
P		182.0	4.7	2.4	0.1	13.6	51.3	9.0	1.2
S		182.0	236.1	135.3	3.5	634.6	57.3	488.5	45.4
Cl		182.0	94.9	197.0	0.2	1097.8	207.6	620.1	0.2
K		182.0	416.5	361.9	40.9	1823.1	86.9	1308.8	118.9
Ca		182.0	2965.8	1794.0	26.3	9957.1	60.5	6761.1	898.3
Ti		182.0	76.3	42.9	2.2	232.9	56.2	169.7	20.7
V		182.0	9.7	5.5	0.6	31.0	56.7	21.8	2.3
Cr		182.0	5.3	3.3	0.5	18.2	61.8	11.7	0.9
Mn		182.0	20.4	10.3	3.7	58.4	50.5	44.2	6.2
Fe		182.0	879.8	459.7	47.6	2816.1	52.2	1845.6	219.5
Co		182.0	45.6	23.7	4.9	149.2	52.0	95.4	12.7
Ni		182.0	11.9	11.9	2.1	82.3	100.1	35.1	2.1
Cu		182.0	7.7	3.9	1.9	36.6	50.2	13.1	3.1
Zn		182.0	81.1	77.4	6.7	642.2	95.5	221.7	24.2
As		182.0	0.7	0.3	0.2	2.0	44.8	1.1	0.2
Se		182.0	1.9	0.9	1.5	5.6	46.0	3.9	1.5
Br		182.0	1.8	0.8	0.7	6.1	44.2	3.1	0.7
Rb		182.0	2.0	1.2	0.6	5.9	58.9	4.4	0.6
Sr		182.0	13.0	7.9	0.0	35.2	61.0	23.9	1.7
Zr		182.0	8.1	3.9	0.7	22.7	48.3	14.3	2.5
Mo		182.0	2.7	1.5	0.0	7.3	57.2	5.6	0.5
Cd		182.0	1.7	1.4	0.2	7.7	86.7	5.1	0.4
Ba		182.0	90.0	51.0	1.3	276.1	56.7	200.2	24.1
Pb		182.0	9.4	5.1	3.6	40.3	54.6	16.3	3.7
EC		182.0	11889.4	4906.9	905.0	22104.0	41.3	19234.2	4225.0
NH ₄		182.0	510.8	739.9	27.6	9130.9	144.8	1183.4	99.6
SO ₄		182.0	5638.4	6738.5	253.7	48891.7	119.5	21957.3	1387.8
NO ₃		182.0	926.0	1361.3	9.1	7699.8	147.0	3856.7	9.1

Table 6. Correlation matrix - Kavadarci dataset

	PM _{2.5}	Na	Mg	Al	Si	P	S	Cl	K	Ca	Ti	V	Cr	Mn	Fe	Co	Ni	Cu	Zn	As	Se	Br	Rb	Sr	Zr	Mo	Cd	Ba	Pb	EC	NH ₄	SO ₄	NO ₃		
PM _{2.5}	1.00																																		
Na	0.68	1.00																																	
Mg	0.62	0.70	1.00																																
Al	0.59	0.64	0.98	1.00																															
Si	0.62	0.65	0.99	0.99	1.00																														
P	0.58	0.67	0.97	0.94	0.96	1.00																													
S	0.37	0.46	0.56	0.58	0.56	0.65	1.00																												
Cl	0.60	0.94	0.43	0.36	0.38	0.41	0.29	1.00																											
K	0.80	0.80	0.63	0.60	0.61	0.60	0.52	0.76	1.00																										
Ca	0.72	0.71	0.89	0.82	0.87	0.84	0.35	0.54	0.67	1.00																									
Ti	0.69	0.66	0.97	0.96	0.98	0.92	0.47	0.41	0.63	0.92	1.00																								
V	0.70	0.66	0.96	0.95	0.97	0.92	0.48	0.41	0.64	0.91	0.99	1.00																							
Cr	0.45	0.42	0.79	0.75	0.77	0.78	0.36	0.17	0.33	0.68	0.78	0.79	1.00																						
Mn	0.69	0.66	0.96	0.93	0.95	0.92	0.45	0.42	0.61	0.92	0.98	0.84	1.00																						
Fe	0.61	0.58	0.95	0.93	0.95	0.92	0.44	0.31	0.50	0.86	0.96	0.89	1.00																						
Co	0.62	0.60	0.95	0.94	0.95	0.91	0.47	0.33	0.52	0.84	0.96	0.88	0.98	0.99	1.00																				
Ni	-0.05	-0.05	0.23	0.18	0.19	0.25	0.03	-0.18	0.10	0.17	0.19	0.62	0.27	0.38	0.35	1.00																			
Cu	0.28	0.30	0.47	0.44	0.45	0.47	0.19	0.16	0.26	0.38	0.43	0.44	0.50	0.48	0.50	0.50	0.35	1.00																	
Zn	0.03	0.03	0.18	0.13	0.14	0.21	0.03	-0.07	-0.05	0.11	0.13	0.15	0.46	0.20	0.28	0.25	0.30	0.25	1.00																
As	0.40	0.46	0.27	0.26	0.25	0.33	0.39	0.46	0.49	0.20	0.25	0.27	0.22	0.27	0.24	0.26	0.02	0.18	0.07	1.00															
Se	0.10	0.14	0.08	0.07	0.07	0.06	0.13	0.14	0.04	0.05	0.06	0.03	0.07	0.05	0.09	0.09	-0.05	0.08	-0.10	0.15	1.00														
Br	0.37	0.43	0.22	0.21	0.20	0.28	0.38	0.44	0.45	0.13	0.20	0.22	0.17	0.21	0.18	0.22	0.00	0.17	0.05	0.95	0.21	1.00													
Rb	0.53	0.55	0.33	0.35	0.34	0.29	0.38	0.56	0.68	0.31	0.34	0.35	0.12	0.34	0.25	0.34	-0.23	0.12	-0.21	0.41	0.36	0.44	1.00												
Sr	0.50	0.54	0.51	0.55	0.53	0.45	0.40	0.43	0.52	0.42	0.53	0.53	0.33	0.53	0.47	0.57	-0.10	0.20	-0.18	0.31	0.37	0.34	0.82	1.00											
Zr	0.56	0.67	0.94	0.91	0.92	0.99	0.73	0.42	0.61	0.78	0.88	0.88	0.75	0.88	0.88	0.88	0.24	0.46	0.20	0.37	0.08	0.33	0.34	0.48	1.00										
Mo	0.36	0.46	0.56	0.58	0.56	0.65	1.00	0.29	0.52	0.35	0.47	0.48	0.36	0.45	0.44	0.47	0.03	0.19	0.03	0.39	0.13	0.38	0.40	0.73	1.00										
Cd	0.81	0.81	0.63	0.61	0.62	0.60	0.52	0.77	1.00	0.67	0.64	0.63	0.62	0.51	0.54	0.17	0.27	-0.06	0.49	0.17	0.45	0.73	0.58	0.61	0.52	1.00									
Ba	0.69	0.66	0.97	0.96	0.98	0.92	0.48	0.42	0.63	0.92	1.00	0.99	0.77	0.98	0.96	0.16	0.42	0.12	0.26	0.06	0.20	0.35	0.54	0.88	0.48	0.88	1.00								
Pb	0.23	0.33	0.24	0.21	0.22	0.26	0.18	0.30	0.29	0.18	0.21	0.24	0.33	0.26	0.27	0.30	0.43	0.30	0.54	0.29	0.13	0.32	0.33	0.28	0.18	0.31	0.21	0.73	1.00						
EC	0.01	-0.12	0.12	0.15	0.13	0.09	0.05	-0.21	-0.14	0.11	0.11	0.29	0.13	0.20	0.22	0.23	0.08	0.13	0.04	0.05	0.05	0.10	0.05	0.12	0.11	-0.02	1.00								
NH ₄	-0.07	-0.07	-0.10	-0.09	-0.10	-0.02	0.23	-0.05	-0.04	-0.13	-0.12	-0.04	-0.11	-0.10	-0.08	0.02	0.01	0.00	0.08	0.11	0.12	0.11	0.07	0.03	0.12	0.13	0.07	1.00							
SO ₄	0.27	0.19	0.27	0.29	0.28	0.24	0.35	0.13	0.33	0.23	0.26	0.27	0.16	0.24	0.21	0.23	-0.02	0.09	0.03	0.08	0.06	0.28	0.27	0.26	0.35	0.33	0.27	0.04	-0.02	0.04	1.00				
NO ₃	0.62	0.53	0.15	0.12	0.13	0.12	0.22	0.64	0.74	0.28	0.18	0.19	-0.04	0.19	0.07	0.09	-0.31	0.03	-0.12	0.41	0.18	0.39	0.57	0.31	0.13	0.21	0.73	0.19	0.39	-0.17	0.05	0.18	1.00		

Temporal variations

Temporal variations of PM2.5 concentrations help clarify the sources and contributing factors that lead to air pollution [15, 16]. Diurnal and seasonal trends can distinguish between traffic-related, industrial, and meteorological impacts on PM2.5 concentrations. A detailed understanding of PM2.5 temporal patterns can inform the development of effective strategies for managing air quality and policies [17]. This includes implementing targeted emission control measures, optimizing monitoring networks, and issuing timely public advisories. Since the temporal variations in PM2.5 are influenced by meteorological factors such as temperature, humidity, and wind patterns [18], comprehending these relationships is essential for assessing the potential impacts of climate change on air quality.

Temporal variations are assessed using gravimetric data in conjunction with real-time data from collocated referent monitoring stations. Modelling was conducted using the Openair R package, which is designed for analysing air quality data, or more broadly, atmospheric composition data. Academics, as well as the public and corporate sectors, widely use the package.

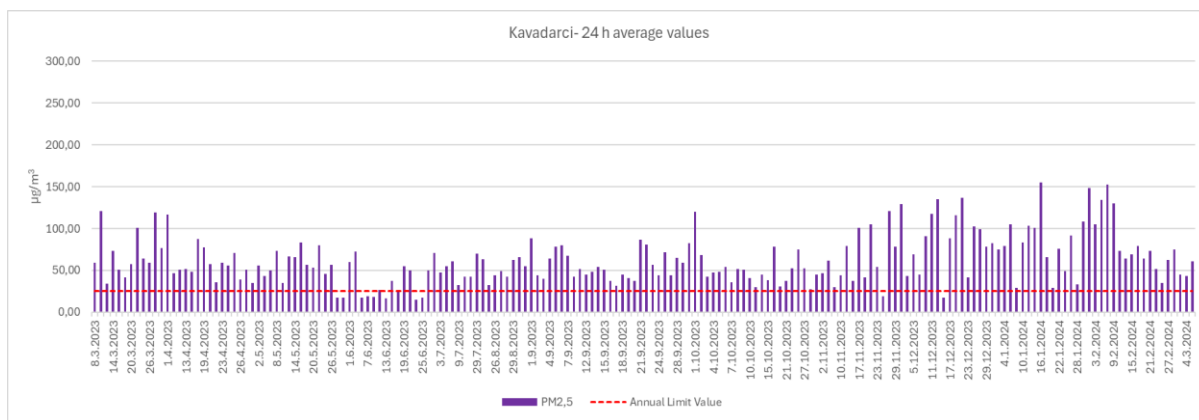


Figure 30. PM 2.5 – daily average concentrations from March 2023 to March 2024

The daily average PM2.5 concentrations measured at the Kavadarci monitoring site show significant daily and seasonal variations, exceeding all European Union limits, targets, and thresholds for human health protection. Daily readings displayed considerable variability, with a standard deviation of $29.1 \mu\text{g}/\text{m}^3$ and a coefficient of variation of 47%. The concentrations ranged from a minimum of $14.7 \mu\text{g}/\text{m}^3$ to a maximum of $154.8 \mu\text{g}/\text{m}^3$, resulting in an average annual value of $62.2 \mu\text{g}/\text{m}^3$, which exceeds the annual threshold limit value of $25 \mu\text{g}/\text{m}^3$ by more than double. The percentage of days exceeding the annual limit for PM2.5 ($25 \mu\text{g}/\text{m}^3$) was an alarming 94.5% (172 out of 182 valid daily readings), with markedly elevated concentrations observed during the colder months ($72 \mu\text{g}/\text{m}^3$) compared to also high levels during the warmer season ($51 \mu\text{g}/\text{m}^3$).

Modelled data, however, show that there is no apparent variation in particulate matter concentration by day of the week or time of day during the spring, summer, or even autumn. On the other hand, although there are no significant differences between the days of the week, winter does exhibit pronounced daily variations with distinct peaks in particulate matter levels at specific times of the day (early morning and late evening). This pattern is often influenced by a combination of meteorological factors, human activities, and local emissions, and is primarily attributed to the increased use of woodstoves and other solid fuel heating methods, which release substantial quantities of particulate matter into the atmosphere. The morning peak typically coincides with the start of daily activities, such as commuting and heightened heating needs, whereas the evening peak corresponds with returning home and subsequent heating activities [19].

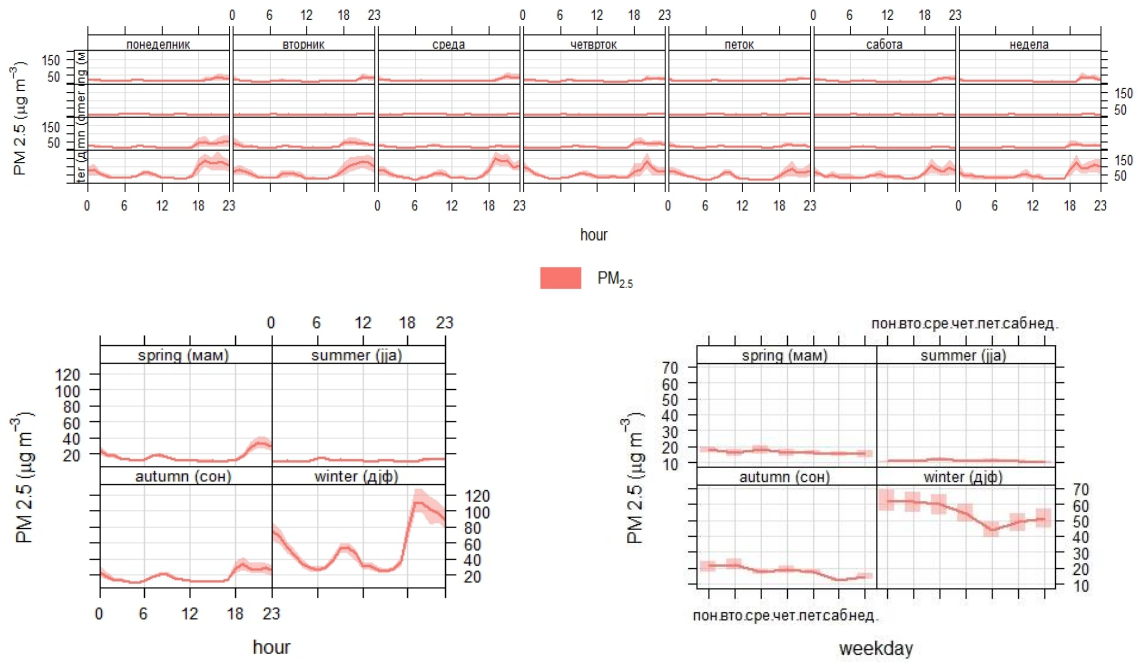


Figure 31. Daily variations in concentrations throughout all days, seasons, and weekdays

Correlation between meteorological conditions and PM concentrations

Bivariate polar plots are an effective analytical tool for understanding the origins and fluctuations of particulate matter, especially finer fractions like PM 2.5. These plots utilize polar coordinates to illustrate the correlation between wind speed and direction, enabling researchers to visualize the impact of these meteorological variables on PM concentrations. The radial axis (circles) commonly represents wind speed, whilst the angular axis signifies wind direction, aiding in the identification of major pollution sources according to their spatial distribution in relation to meteorological conditions.

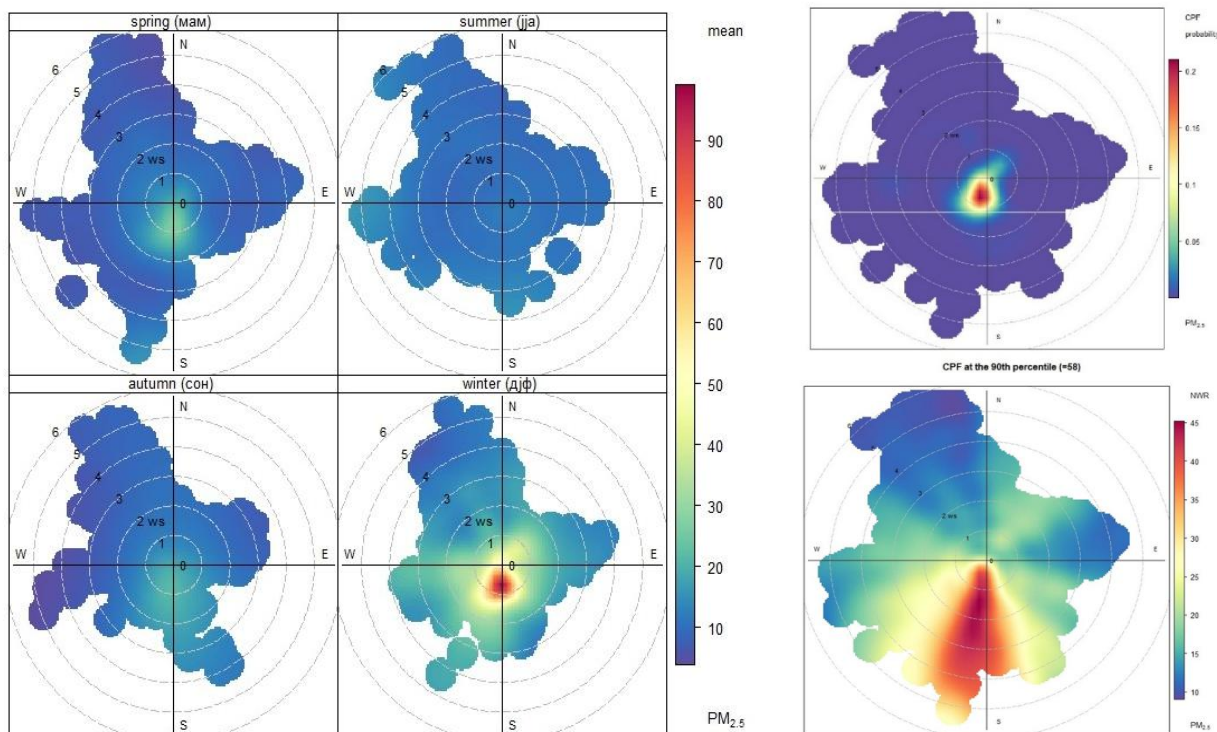


Figure 32. Bi-variate (seasonal), CPF and non parametric polar plots

Polar plots for the Kavadarci area show that changes in concentration are mainly affected by local sources, as higher PM levels are mostly seen during quiet winter weather, which usually has low wind speeds below 1 m/s. The conditional probability function supports this assertion by showing that higher particulate matter levels are mainly linked to low wind speeds, suggesting that these levels originate from local or nearby sources.

Additionally, non-parametric wind regression (NWR) plots were used as a different way to better understand where pollution comes from in relation to wind patterns. This method uses nonparametric kernel smoothers that give more importance to pollution levels based on how close they are to certain wind speeds and directions. The analysis indicates that most of the pollution is associated with weak winds blowing from the south, suggesting that the pollution is local. Given that this direction corresponds with the urban area of the city, it implies that the sources of pollution are located within the city limits.

PM 2.5 chemical composition

The chemical compositions of PM2.5 differ across Europe and on average, Central Europe has more carbonaceous matter in PM2.5, North-western Europe has more nitrate, and southern Europe has more mineral dust in all fractions [20].

The contribution of mineral (soil) particles measured in Kavadarci is significantly higher than the values recorded in Skopje and is within the range identified in certain regions of Southern Europe, achieving an annual average of around 9% [20, 21]. Elements like Mg, Al, Si, Ca, Ti and Fe, usually used as tracers for soil dust, are well correlated, indicating a common source for these elements and providing clear identification of this source in subsequent factor analysis.

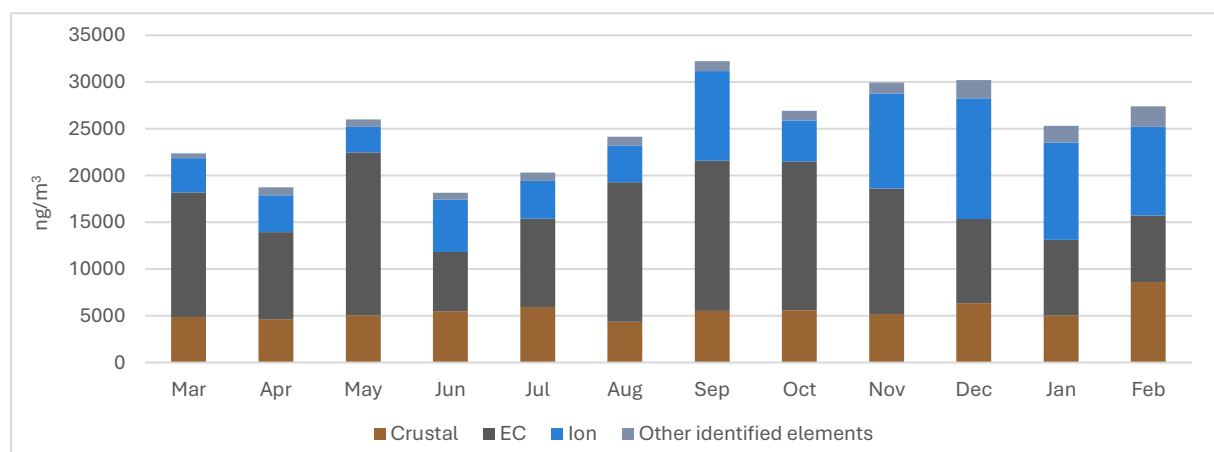


Figure 33. Major components and elemental groups identified

Sea salt contributions are negligible, as would be expected for a typically continental location. The contributions of ions (sulphates and nitrates) are markedly lower than those documented throughout Europe, with a combined contribution of 11% falling within the range of values observed in Skopje [20, 21]. This may be attributed to several factors; however, it is important to note the relatively low average concentrations of gaseous precursors such as sulfuric and nitrous oxides.

Elemental carbon (EC) contributions in the urban area of Kavadarci exceed European averages, with an average of 19%. This figure is slightly lower than that observed in Skopje and somewhat higher than values recorded in Central Europe. This discrepancy likely reflects the local sources of emissions, with wood combustion identified as the most significant single source of

particulate matter. Traffic emissions, particularly exhaust from service and older diesel-powered vehicles, can significantly impact this situation.

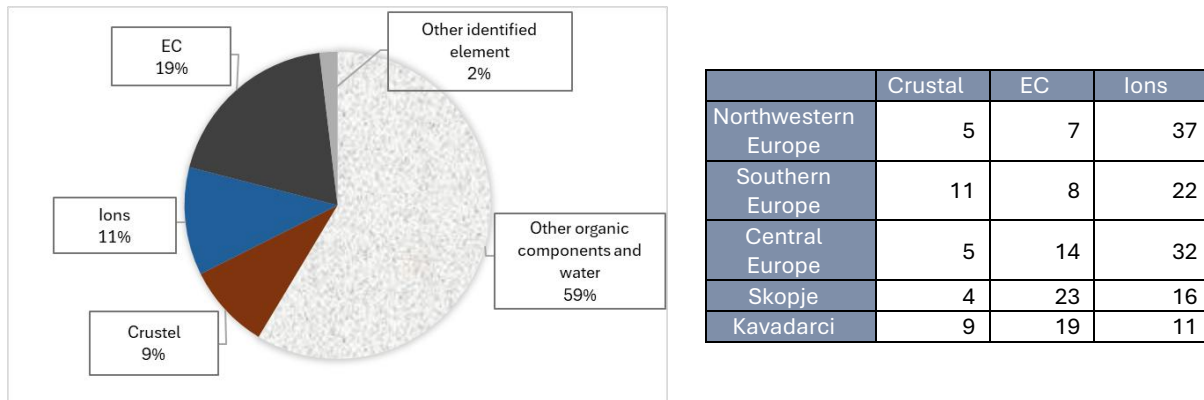


Figure 34. Contribution of major particulate matter components [20, 21]

Assessment of regulated metals, specifically lead, arsenic, cadmium, and nickel, was conducted only for those metals that successfully underwent external quality assessment procedures, encompassing only lead and nickel. The results for arsenic and cadmium are available; however, they are excluded from direct comparison due to significant uncertainty associated.

It was determined that average annual concentrations of lead and nickel found were within the annual limit threshold values as specified in Directives 2008/51/EC and 2004/71/EC. However, the concentrations of Ni were found above the lower assessment target and therefore further assessment for compliance is required. Significantly elevated average annual concentrations of nickel predominantly arise during arid months, so suggesting that the resuspension of mineral dusts is a principal source of this element.

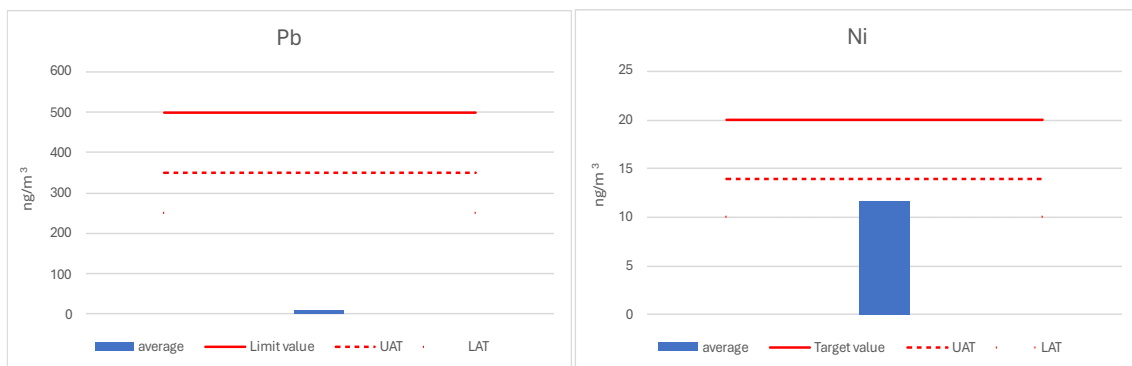


Figure 35. Average monthly concentrations of lead (Pb) and nickel (Ni) in Kavadarci

5. Positive Matrix Factorisation

Environmental monitoring data are increasingly being handled in terms of mathematical models, which allow for the management of a variety of datasets with multiple observations to be performed. Different modeling techniques are available depending on the type of known information (input data) and the sort of results that would be obtained (output data) that are desired.

Source allocation (SA) is the practice of obtaining information about pollution sources and the amount of pollution that each source contributes to the level of ambient air pollution. Emission inventories, source-oriented models, and receptor-oriented models are three ways that can be used to do this task.

Recent years have seen the rise in importance of receptor-oriented models (also known as receptor models (RMs)) in environmental sciences, which are used to elicit information from datasets that contain a number of features (chemical or physical qualities) associated with the measured samples. For example, they can be used to assess the contribution of contamination and pollutant sources in various types of samples, starting with the information provided by the samples (which is recorded at the monitoring site) and progressing to the point of effect, or receptor.

Receptor models are also known as multivariate methods because they are used to analyze a data set containing a large number of numerical values as a whole. Receptor models, to be more precise, are mathematical methodologies for measuring the contribution of sources to samples based on their composition or fingerprints. To separate impacts, the composition or speciation is identified using media-specific analytical methods, and key species or combinations of species are required. A speciated data set can be considered of as a data matrix X with i by j dimensions, in which i samples and j chemical species were measured with u uncertainty.

The goal of receptor models is to solve the chemical mass balance (CMB) in Equation 1, between measured species concentrations and source profiles, where p is the number of factors, f is each source's element profile, g is each factor's mass in each sample, and e_{ij} is the "remaining" for each element/sample.

$$x_{ij} = \sum_{k=1}^p g_{ik} f_{kj} + e_{ij} \quad (1)$$

A dataset containing a vast amount of data consisting of chemical elements (such as elemental concentrations) acquired from a large number of observations (samples) is required to find the answer. The larger the data matrix, the more likely the model is to uncover separate factors that can be used as sources. The number of samples required can vary depending on prior knowledge of the sources and the RMs methodology chosen (e.g., CMB vs. PMF).

If the number and nature (composition profiles/fingerprints) of the sources in the study area are known, then the only unknown term of equation (1) is the mass contribution of each source to each sample. To solve the chemical mass balance and to elicit information on sources type, number and contribution starting from observations (i.e. element concentrations data set) at receptor site, different factor analysis methods (multivariate methods) have been developed. Common factor analysis methods used include Principal Component Analysis (PCA), Unmix, Target Transformation Factor Analysis (TTFA), Positive Matrix Factorization (PMF) and Multilinear Engine (ME).

Dr. Pentti Paatero (Department of Physics, University of Helsinki) created Positive Matrix Factorization (PMF) in the mid-1990s to establish a new method for the analysis of multivariate data that addressed several drawbacks of the PCA.

PMF uses error estimates to weight data values and imposes non-negativity constraints in the factor computational process. The algorithm accomplishes weighted least squares fit with the objective of minimizing Q, a function of the residuals weighted by the uncertainties of the species concentrations in the data matrix. The PMF factor model can be written as $X = G \cdot F + E$, where X is the known n·m matrix of the m measured chemical species in n samples. G is an n·p matrix of factor (source) contribution in every sample (time series). F is a p·m matrix of factor compositions (factor profiles). G and F are factor matrices to be determined and E is defined as a residual matrix, i.e. the difference between the measured X and the modeled Y = G·F.

In this study, the free software US-EPA PMF 5.0 version 5.0.14 [22], implementing the ME-2 algorithm developed by Paatero (1999), was used.

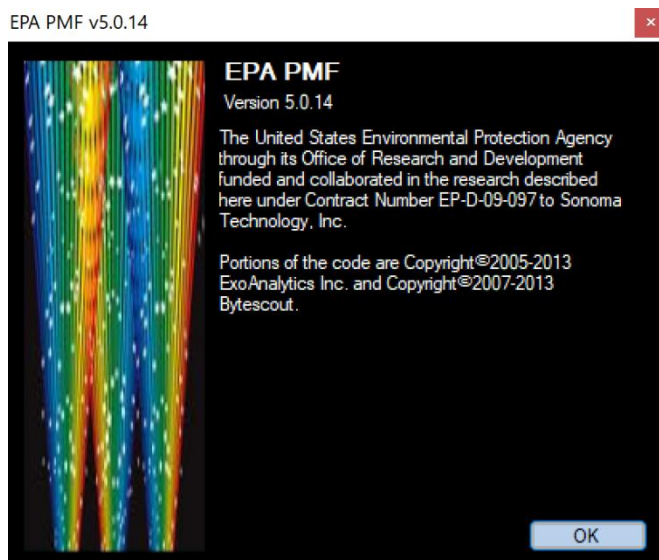


Figure 36. Free software US-EPA PMF 5.0 version 5.0.14 – splash screen

PMF was first employed in studies of air pollution and source apportionment [23, 24] as well as precipitation investigations [25]. Air quality and source apportionment applications [26, 27] have gained rapid popularity in recent years, but PMF has also been used on lake sediments [28], wastewater [29, 30] and soils [31]. This multivariate factor analysis tool has been used to analyze a variety of data, including 24-hour speciated PM2.5, size-resolved aerosol, deposition, air toxics, high time resolution measurements from aerosol mass spectrometers (AMS), and volatile organic compound (VOC) data.

The use of known experimental uncertainties as input data allows for individual handling of matrix members and can handle missing or below-detection-limit data, which is a prevalent feature of environmental monitoring. Because the PMF results are quantitative, it is feasible to determine the composition of the sources determined by the model.

Equation 2 was used to determine the uncertainty of the utilized method for each element separately, and Equation 3 was used to determine the uncertainty of the instrument for each element separately:

$$u = \sqrt{U_{instrument}^2 + U_{CRM}^2 + U_{sampling}^2} \quad (\%) \quad (2)$$

$$U_{instrument} = \frac{STDEV}{average} * 100 \quad (\%) \quad (3)$$

Where $U_{instrument}$ - uncertainty of the used instrument, U_{CRM} - uncertainty of the used certified referent material, $U_{sampling}$ - uncertainty of the sampling.

Before data processing, various basic statistical tests—such as dispersion, distribution, correlation matrices, linear regression, and time trends—were conducted to examine the relationships among the variables.

5.1. Input data and PMF model setting

Species lists included water-soluble ions NH_4^+ , SO_4^{2-} , NO_3^- , elemental carbon (EC), and following elements; Na, Mg Al, Si, Ca, K, Ti, Fe, P, S, Cl, V, Cr, Mn, Co, Ni, Cu, Zn, As, Se, Br, Rb, Sr, Zr, Mo, Cd, Ba and Pb.

Following the EU protocol for receptor models [32], the data were initially processed to remove values that could potentially degrade the quality of the analysis. To validate the data and identify atypical values when compared to the rest of the dataset, scatter plots and time series analysis were employed. After data validation, the original datasets included 32 species and 182 daily samples.

As recommended in EU protocol for receptor models [32], data below the limit of detection (LOD) were substituted by half of the LOD and the uncertainties were set to 5/6 of the LOD. Missing data were substituted by the geometric mean of the measured concentrations and the corresponding uncertainties were set as 4 times this geometric mean [33].

Species with high noise were down-weighted based on their signal-to-noise (S/N) ratio to reduce the influence of poor variables on the PMF analysis. Species with S/N lower than 0.5 were considered as bad variables and excluded from the analysis, and species with S/N between 0.5 and 1 were defined as weak variables and down-weighted by increasing the uncertainty as recommended in the PMF users guideline. The elemental concentration and uncertainties for the dataset are set as weak for Ni, As and Cd. The EC also was set as a weak although S/N was above 8. Although with high signal to noise ratio, PM 2.5 was set as total (week) variable in order to reduce influence on profiles contribution.

The used procedure more detailed is described in Source Apportionment Study for Skopje urban area –identification of main sources of ambient air pollution [34].

5.2. Factor attribution to sources

Final PMF solution for Kavadarci datasets included 6 factors. Factors were attributed to their sources through a quantitative and qualitative comparisons of the factor chemical profile with PM profiles reported EC-JRC SPECIEUROPE data base and profiles from previous source apportionment studies available in the literature. In addition, the standardised identity distance (SID) and the Pearson coefficient, expressed as Pearson distance ($\text{PD} = 1 - r$), were used to calculate the similarity between the factors and the reference source profiles available in the public datasets: EC-JRC SPECIEUROPE and US-EPA SPECIATE [35]. The Delta SA tool [10] was used to complete the work.

Factors that were identified in municipality of Kavadarci are as follows: biomass burning, traffic, fuel and residual oil, road and soil dust, open fire and waste burning and secondary aerosols.

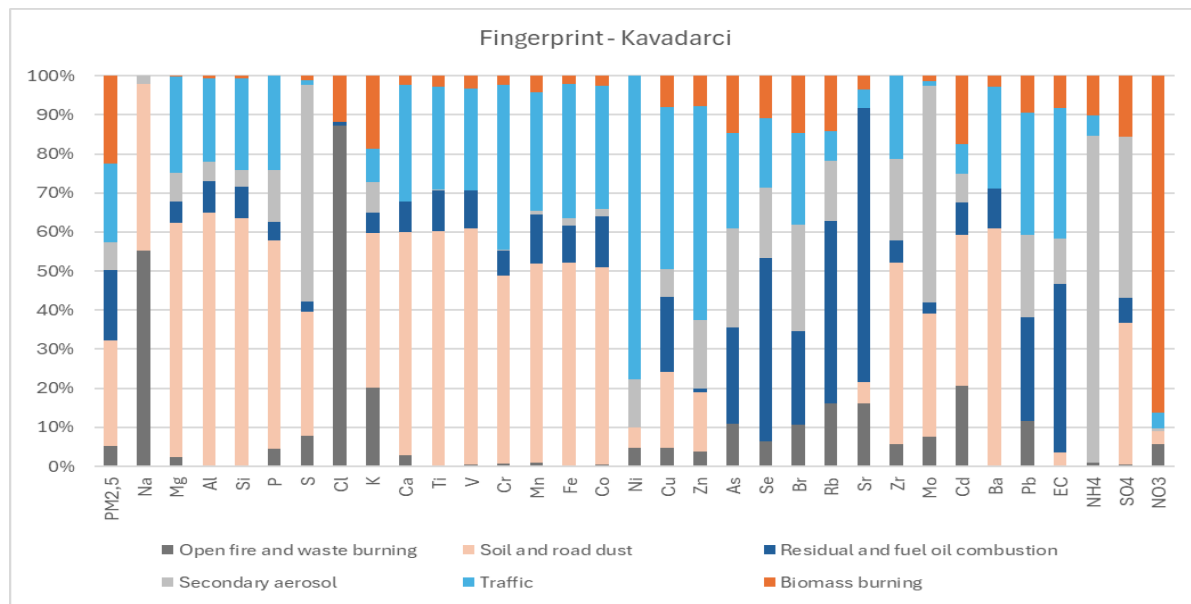


Figure 37. Factor fingerprint for Kavadarci

Biomass burning incorporates emissions from different types of woodburning stoves and boilers used mostly in residential heating. Key species found in this factor include EC, K, Cl, NO_3^- and Rb. K is produced from the combustion of wood lignin [36, 37]. Although this element can be emitted from other sources, such as soil dust [38], K has been used extensively as an inorganic tracer to apportion biomass burning contributions to ambient aerosol and was associated with biomass burning in PMF source profiles in Tirana, Skopje, Athens, Belgrade, Banja Luka, Debrecen, Chisinau, Zagreb and Krakow [39].

Cl can be emitted from biomass burning and also from coal combustion, especially during the cold period [40]. It is also associated with biomass burning in PMF source profiles in Belgrade and Banja Luka [39]. In addition, NO_3^- , and NH_4^+ also contributed significantly to the biomass burning factor. Biomass burning is an important natural source of NH_3 [41] which rapidly reacts with HNO_3 to form NH_4NO_3 aerosols. The presence of NH_4NO_3 aerosols in biomass burning plumes, has also been reported previously [41, 42].

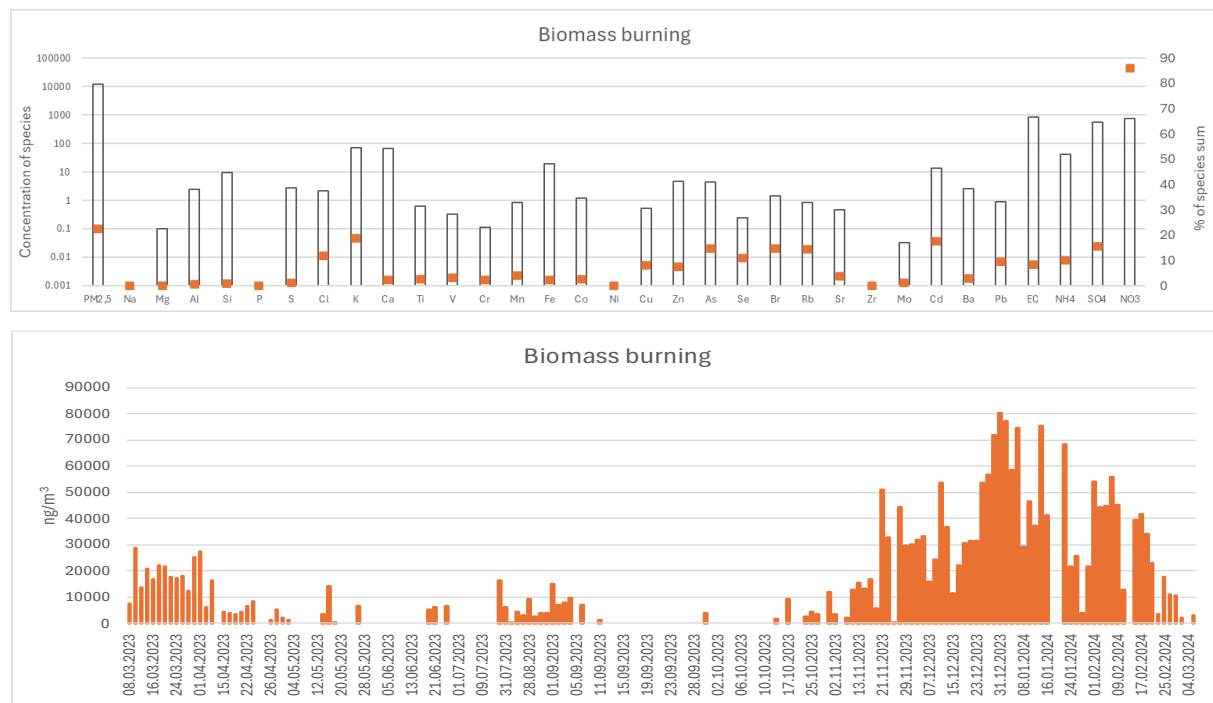


Figure 38. Biomass burning factor profiles in Kavadarci

Evaluation of seasonal pattern of this factor clearly confirm attribution of this factors to biomass burning emissions that usually occur only during the cold months.

Traffic includes particles from several different sources including vehicles exhaust, mechanical abrasions of brakes and tires, road (resuspended) dust and road salting. All sources associated have their own specific fingerprints, and can be identified by EC, Ba, Cu, Mn, Pb and Zn, as well as crustal species like Mg, Al, Si, Ca, Fe, and Ti, or Na and Cl in the case of winter road salting.

The vehicle exhaust, including diesel and gasoline, consist high percentage of organic and elemental carbon, Fe, Pb, Zn, Al, Cu and sulphate. Similar species were also associated with traffic in PMF source profiles in most European and Central Asia urban areas [39].

Zn is a major additive to lubricant oil. Zn and Fe can also originate from tire abrasion, brake linings, lubricants and corrosion of vehicular parts and tailpipe emission [43-46].

As the use of Pb additives in gasoline has been banned, the observed Pb emissions may be associated with wear (tyre/brake) rather than fuel combustion [47].

Fe and Al is likely associated with vehicles part wear, such as tyre/brake wear and road abrasion, and are common species in case sampling sites are located close to major roads.

These results indicate the contribution of both exhaust and non-exhaust traffic emissions to various factors associated with traffic. The elemental composition of particulate emissions linked to traffic can vary significantly due to differences in traffic volume and patterns, vehicle fleet characteristics, climate, and the geology of the region [48]; however, similar elements (Cu, Mn, Zn, Pb, Fe, and EC) have been identified as key species in PMF source profiles across most urban areas in Europe and Central Asia [39].

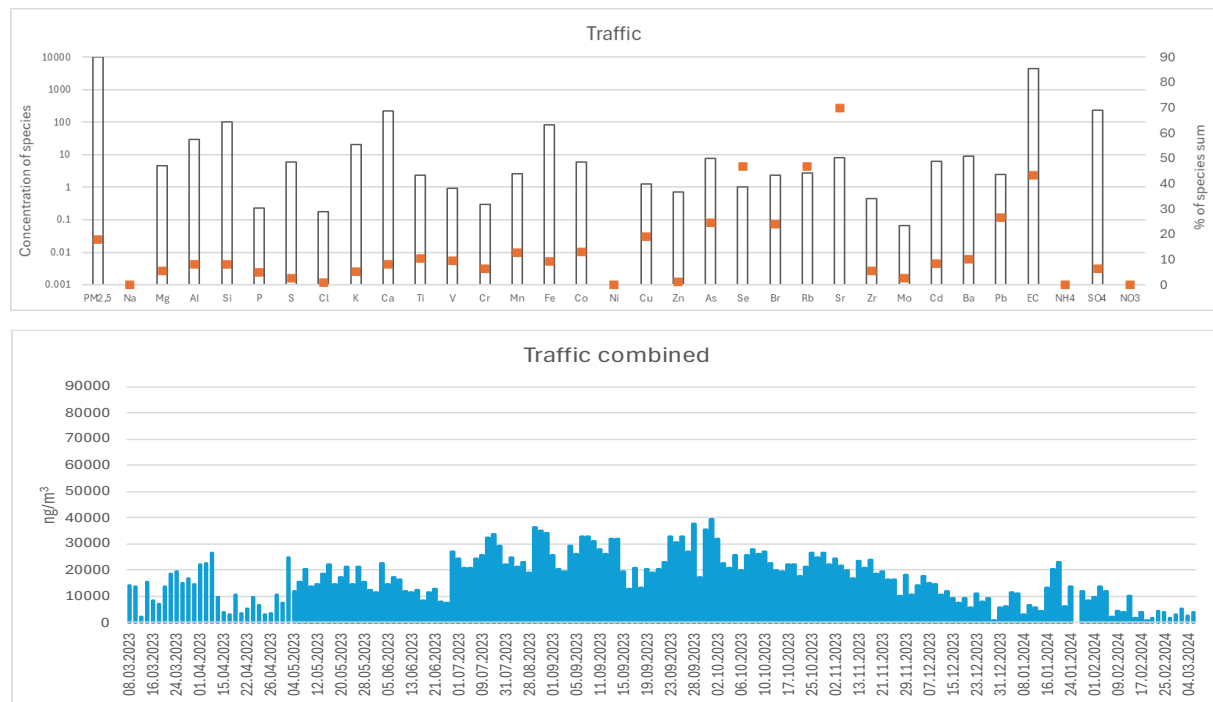


Figure 39. Traffic associated factors for Kavadarci dataset

Fuel and residual oil combustion is a stand-alone factor that includes emissions from a wide range of sources, the majority of which are larger buildings heating systems (schools, hospitals, and other public institutions), industrial combustion emissions and to some extent older diesel-powered vehicles emissions, principally composed of EC, V, Cd and Ni [41, 42].

Organic carbon, sodium, and water-soluble ions including nitrates and sulphates are common key species for fuel oil emissions. The presence of V and Ni is also common marker. Water-soluble ions, V, Fe, and Ni are also important species for residual oil combustion, but increased quantities of elemental carbon, rather than organic carbon, are common for this source.

Vanadium, either alone or in conjunction with nickel, is a prevalent marker in PMF source profiles, in most European and Central Asian urban areas [39].

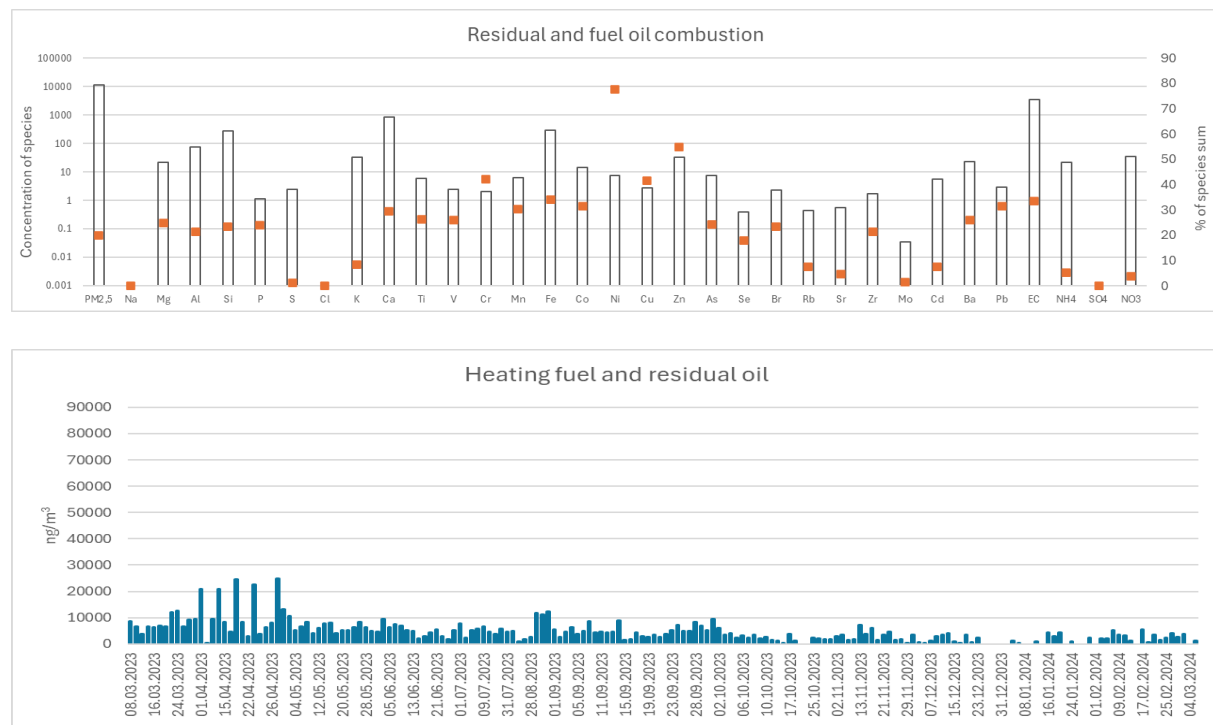


Figure 40. Fuel and residual oil factor profiles

Soil or mineral dust usually originates from construction/demolition activities, dust resuspension and wind erosion processes. This source is commonly identified with so called crustal elements like Mg, Al, Si, Ca, Fe and Ti [49]. Silicon and Ca are usually most abundant elements, followed by Fe, Al, Mg, and Ti with variations due to local geology.

Other research studies also reported significant contribution of soil dust to PM2.5 mass, suggesting that soil dust is an important contributor to PM2.5 mass especially in summertime [50, 51]. Similar elements (Ca, Fe, Al, Si, Ba, Na and Ti) were identified as key species in PMF source profiles in most European and Central Asia urban areas [39].

Silicon and calcium are also prevalent species in the construction related source's chemical profile. Chemical profile of construction source also includes Si, Ca, Al and Fe, but also OC, EC and sulphates have significant contribution.

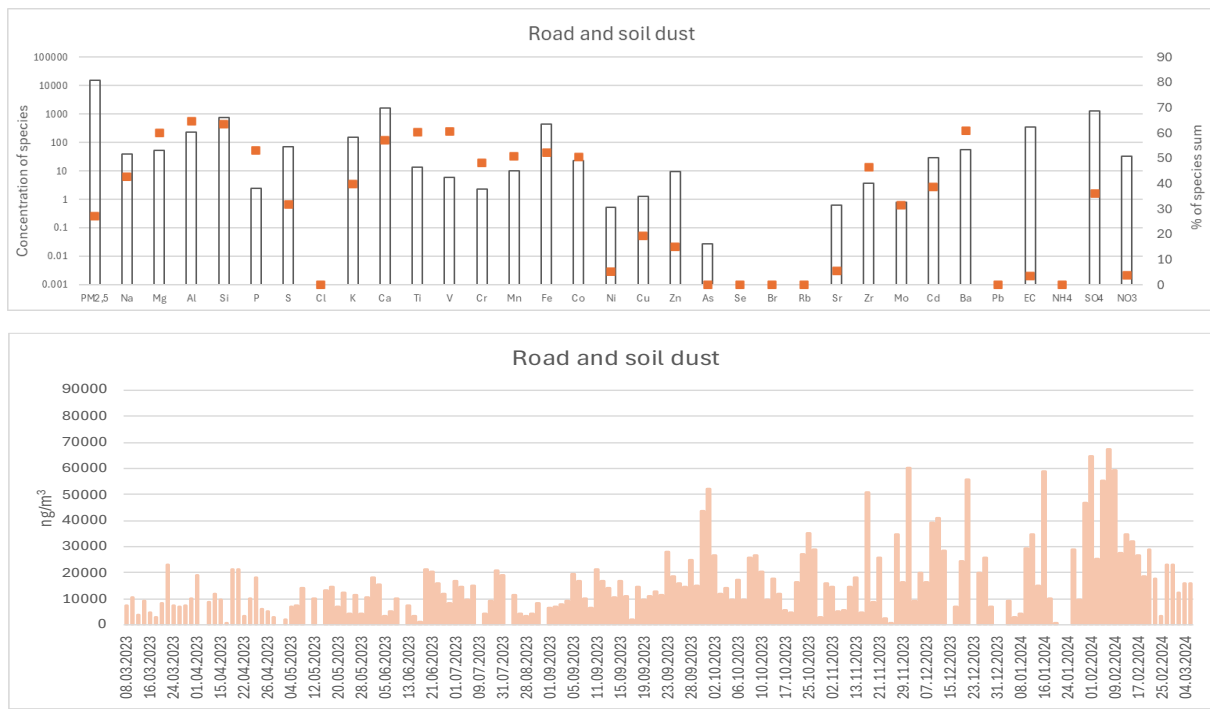


Figure 41. Mineral dust factor profiles

All types of low efficiency burning of agricultural and garden waste, as well as other types of waste, are classified as open fire burning. This factor is identified by high contribution Cl, As, Cd and Rb, but also includes some specific metals like Pb, Cu and Ni. Elemental carbon, Br, Co, V, Ti, and As were also found as important species in an analysis of agricultural waste open burning profiles, conducted in the Thessaloniki area in Northern Greece (SPECIEUROPE data base). According to Lemieux [52] depending on the source, varying amounts of metals such as lead (Pb) or mercury (Hg) may be emitted. Polychlorinated dibenzo-p-dioxins and polychlorinated dibenzofurans (PCDDs/Fs) or polychlorinated biphenyls (PCBs) can be emitted as well.

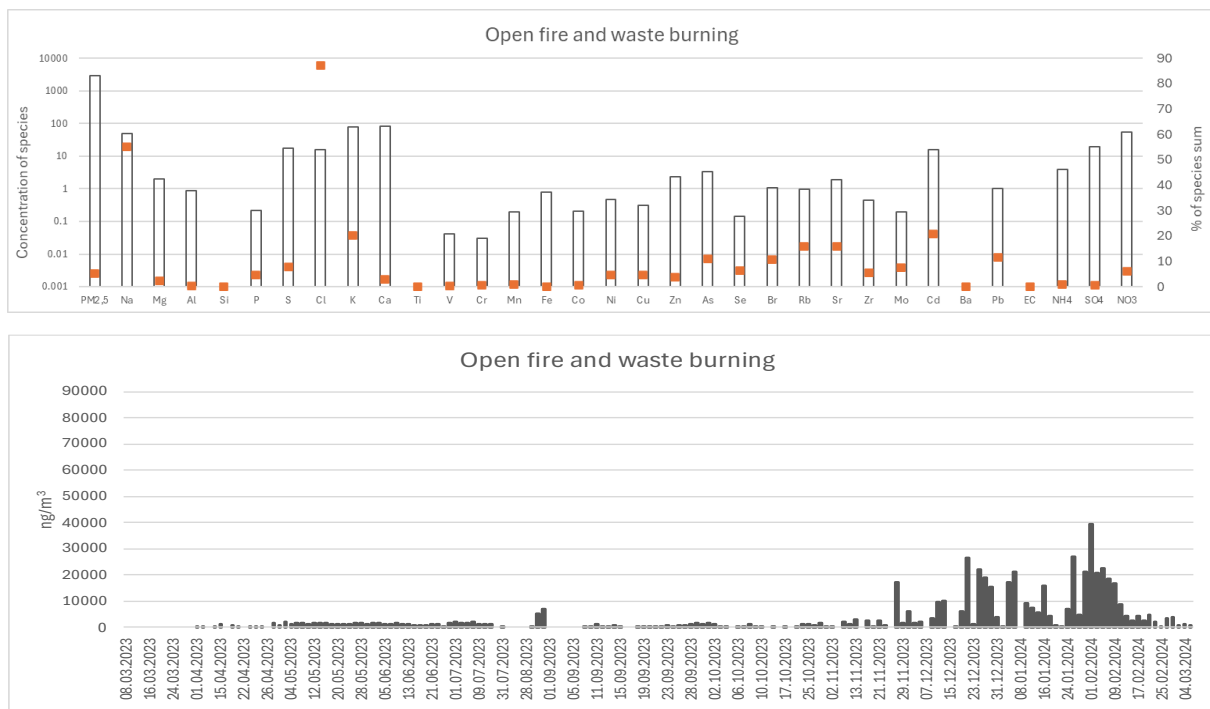


Figure 42. Open fire burning factor profile

Secondary aerosols contribute significantly during the coldest and warmest months, when there are elevated levels of gaseous precursors in the winter and high temperatures in the summer.

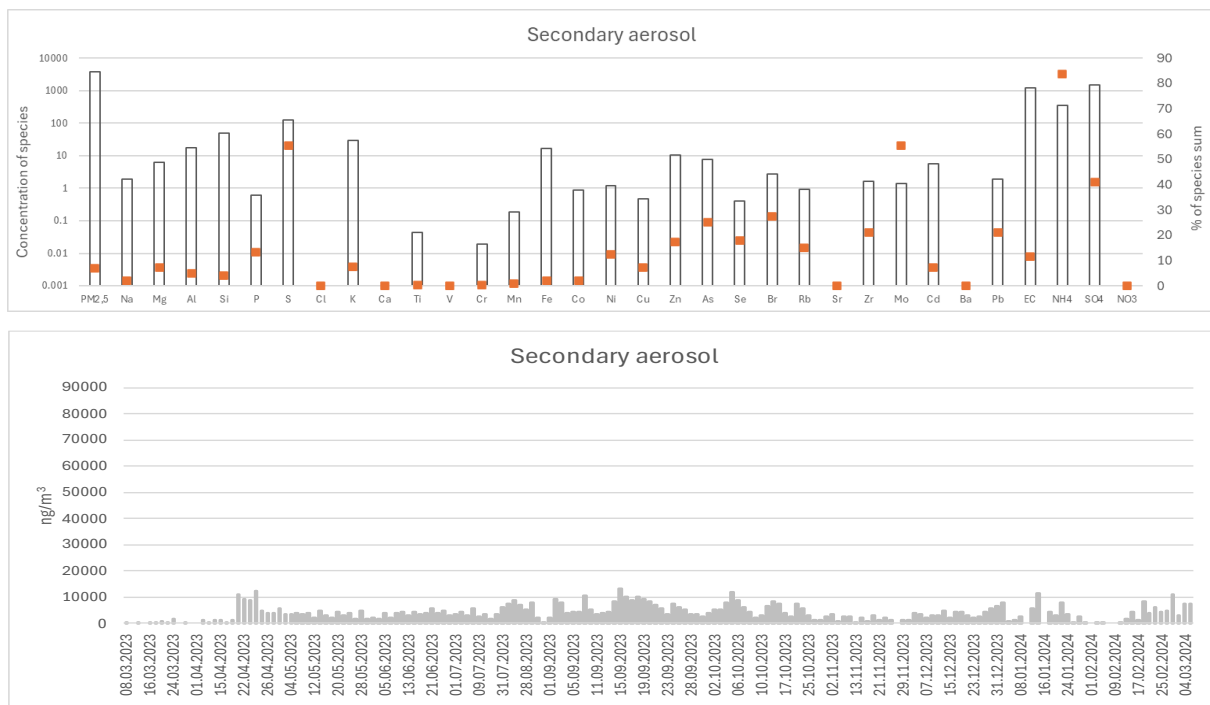


Figure 43. Secondary Aerosols factor profile

5.3. Sources Contribution

The contribution of each source to the total particle mass (PM 2.5) was determined using data from measurements and modelling exercises. The primary sources identified for Kavadarci include biomass burning, open fires and waste burning, traffic, secondary aerosols, road and soil dust, and fuel and residual oil combustion. The traffic contribution was determined by combining modelled values from two identified sources: traffic and the combustion of fuel and residual oil. Because of the resemblance in exhaust emissions from older diesel vehicles and fuel oil-burning boilers, a significant amount, 70 %, of fuel oil contributions during warmer periods are attributed to traffic sources.

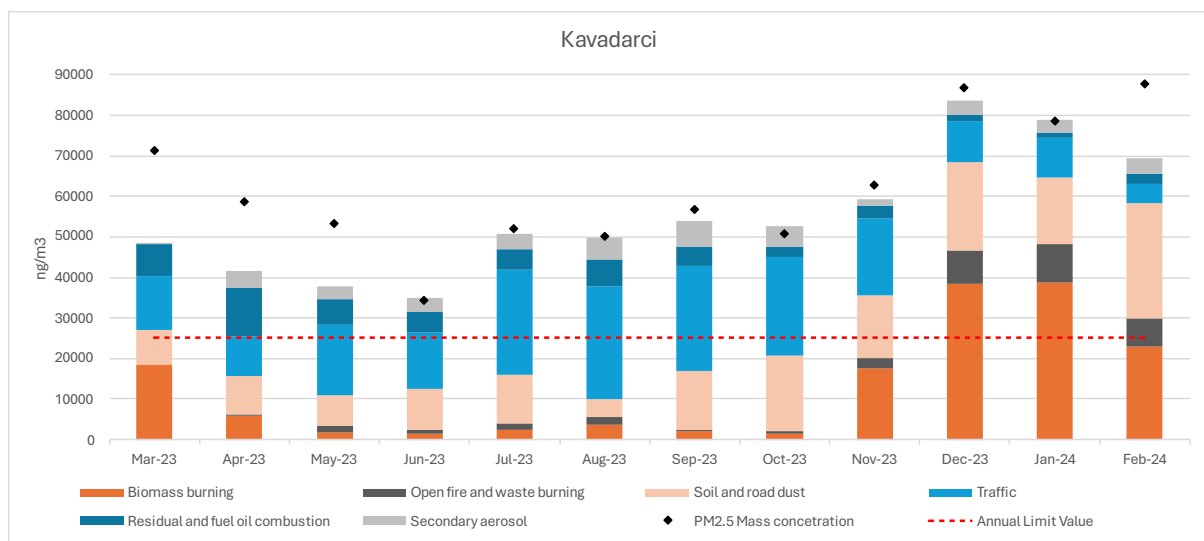


Figure 44. Average monthly contributions to total particulate mass (PM 2.5) – Kavadarci

Biomass burning was a one of the most significant air pollution sources during the winter months, with the biggest contribution to total particle mass occurring in November, December, January, February, and March, while having minimal impact during the summer months. Biomass burning mostly belongs to residential heating; however, it also includes biomass burning in bakeries,

restaurants, and small industrial establishments that utilize wood for heating or generating thermal energy for their operational processes. The average monthly contribution of biomass burning over the winter season ranged from 17.5 to 38.8 $\mu\text{g}/\text{m}^3$. This source alone, during the winter season, exceeds the yearly limit value for PM 2.5, set at 25 $\mu\text{g}/\text{m}^3$. The relative contributions (%) of biomass burning to total particle mass demonstrate significant seasonal variability, with this source accounting from 30 to 50 % during winter months, and although entirely seasonal, biomass burning accounts for a significant annual relative contribution of 23%.

Annually, traffic represents the primary air pollution source, demonstrating a steady contribution throughout the year, with a notable increase during the summer and fall months, ranging from 4.6 to 27.7 $\mu\text{g}/\text{m}^3$. The annual relative contribution of traffic constituted 31 % of the total particulate mass (PM 2.5), with monthly relative contributions varying between 5.3 % and 55.1 %. This source includes emissions resulting from vehicles exhaust, brake and tire wear, in addition to the combustion of oil in older diesel engines, such as those found in tractors, trucks, and older passenger vehicles lacking exhaust control devices.

Road and soil dust, additionally referred to as mineral dust, comprises particulate matter primarily originating from construction activities and the resuspension of deposits on roadways. This source significantly contributes to total particulate mass (PM2.5), with an increasing contribution during dry seasons, ranging from 4.5 to 28.6 $\mu\text{g}/\text{m}^3$. The monthly contributions from this source vary between 8.9 % and a significant 36.2 %, but the annual relative contribution attains a notable 25 %. The substantial contribution may also be attributed to road rehabilitation activities conducted near the monitoring site.

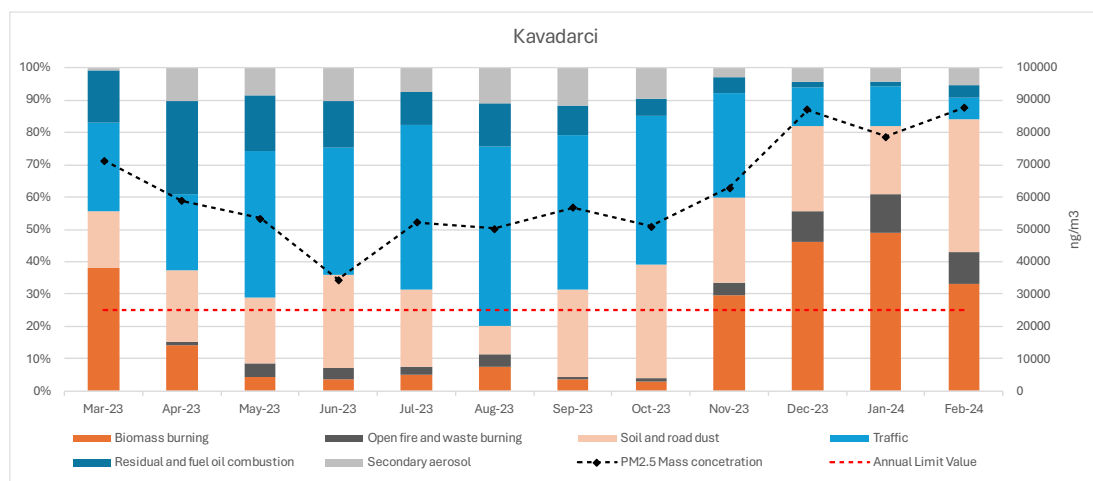


Figure 45. Relative monthly contribution – Kavadarci

Combustion of fuel and residual oil mainly comes from furnaces for heating public facilities and buildings (kindergartens, schools, hospitals), as well as in industrial facilities for heat production or some other technological processes. Fuel and residual oil contribute from 1.1 and 11.9 $\mu\text{g}/\text{m}^3$ to total particulate mass. This source occurs consistent over the year. Annual relative contribution of fuel and residual oil combustion accounted for 9 % of the total particulate mass (PM 2.5) mass. Relative monthly contribution ranged from 1.5 to 20.3 %.

Open fires and waste burning include the combustion of crop residue, agricultural and garden waste materials, as well as landfill fires and wildfires. This factor also includes the combustion of diverse waste materials in household stoves or small industrial boilers and is predominantly observable during the spring and early summer months, with an increased contribution in the autumn and winter periods. The monthly contribution from this source reaches up to 12 %, while the annual contribution is 5 %.

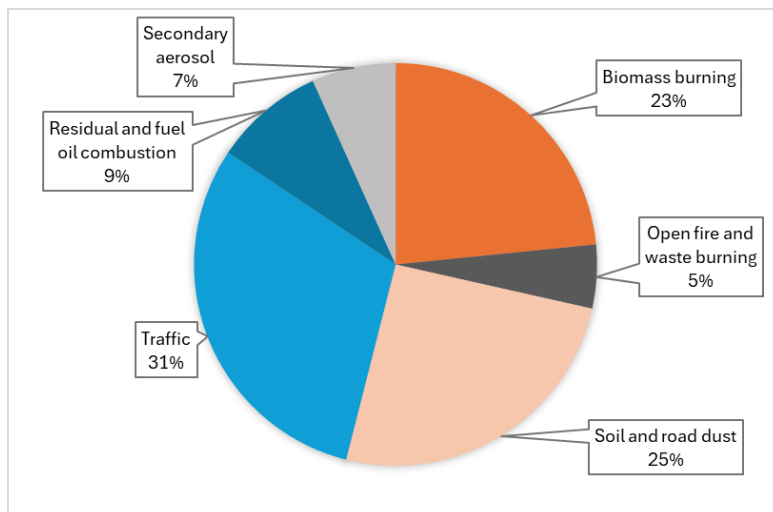


Figure 46. Relative annual contribution of PM 2.5 sources at Kavadarci

Secondary aerosols are particles formed by chemical reactions in the atmosphere, influenced by sunlight, ozone, and humidity. Secondary aerosols have the biggest contribution during the coldest and hottest months, probably because there are more gas precursors in winter and chemical reactions from high temperatures in summer. The contribution of secondary aerosols ranges from 0.3 to 6.4 $\mu\text{g}/\text{m}^3$. The annual relative contribution of secondary aerosols was 7 % of the total particle mass (PM2.5), with monthly contributions displaying significant variability, ranging from 0.4 % to 11.2 %.

6. Conclusions and recommendations

The urban region of Kavadarci suffers poor air quality over an extended period. Particulate matter (PM 10) concentrations continuously exceed established threshold limits. Between 2017 and 2021, Kavadarci's average annual PM10 concentrations and the number of exceedances of the 24-hour limit value have continuously exceeded the recommended levels.

The AMBICON Laboratory conducted this Source Apportionment Study to gather information on pollution sources and their contributions to ambient air pollution in Kavadarci. The activities followed the strict guidelines in the European handbook on air pollution source apportionment using receptor models (Revised edition 2019, JRC) and included a year-long program for collecting and analyzing air samples, which helped create a complex model to identify pollution sources. The sampling program started on March 8, 2023, and until the end of April 2024, 182 samples were collected, with a 24-hour sample being taken every other day. The sampling process was executed in strict compliance with the standard gravimetric measurement method for determining the mass concentration of PM10/PM2.5 suspended particulate matter (EN 12341:2014). Energy dispersive X-ray fluorescence (ED-XRF) was used to analyze the elements, an optical transmissometer measured the amount of elemental carbon, and spectrophotometry helped identify water-soluble ions.

The daily average PM2.5 concentrations measured at the Kavadarci monitoring site exhibit significant daily and seasonal variations, exceeding all national and European Union limits, targets, and thresholds for human health protection. Concentrations measured ranged from a minimum of $14.7 \mu\text{g}/\text{m}^3$ to a maximum of $154.8 \mu\text{g}/\text{m}^3$, resulting in an average annual value of $62.2 \mu\text{g}/\text{m}^3$, which exceeds the annual threshold limit value of $25 \mu\text{g}/\text{m}^3$ by more than double. The percentage of days surpassing the annual limit for PM 2.5 ($25 \mu\text{g}/\text{m}^3$) was an alarming 94.5 % (172 out of 182 valid daily readings).

Modelled data, show that there is no apparent variation in particulate matter concentration by day of the week or time of day during the spring, summer, or even autumn. On the opposite side, although there are no significant differences between the days of the week, during the winter there are expressed daily variations with distinct peaks in particulate matter levels at specific times of the day (early morning and late evening). This pattern is often influenced by an interaction of meteorological factors, anthropogenic activities, and local emissions, and is predominantly attributed to the increased utilization of woodstoves and other solid fuel heating means, which discharge substantial quantities of particulate matter into the atmosphere.

Polar plots generated for the Kavadarci area demonstrate concentration variations influenced from local meteorological conditions, notably indicating that elevated PM concentrations are exclusively observed during the winter season and are predominantly linked to low wind speeds (1 to 2 m/s), blowing mostly from the south. Furthermore, non-parametric wind regression (NWR) plots also demonstrates that the majority of pollution originates from the south, a direction that aligns with the urban area of the city, suggesting that the sources are situated within the city limits.

Using the data from measurements and modelling exercise, contribution of each source to total particulate mass (PM 2.5) was calculated. The major sources identified for Kavadarci include biomass burning, open fire and waste burning, traffic, secondary aerosols, road and soil dust, and fuel and residual oil burning.

On annual level, traffic represents the primary air pollution source, demonstrating a steady contribution throughout the year, with a notable increase during the summer and fall months. The annual relative contribution of traffic constituted 31 % of the total particulate mass (PM 2.5),

with monthly relative contributions varying between 5.3 % and 55.1 %. Biomass burning is also one of the most important sources with relative contribution to total particulate mass accounting from 30 to 50 % during winter months, and although entirely seasonal, biomass burning accounts for a significant annual relative contribution of 23 %. Road and soil dust, additionally referred to as mineral dust, also significantly contributes to total particulate mass (PM2.5), with an increasing contribution during dry seasons, ranging between 8.9 % and a significant 36.2 %. Open fires and waste burning include the combustion of crop residue, agricultural and garden waste materials, as well as landfill fires and wildfires. This factor also includes the combustion of diverse waste materials in household stoves or small industrial boilers, therefore having increased contribution in the autumn and winter periods. The monthly contribution from this source comes up to 12 %, while the annual contribution is 5 %.

It is evident that, due to its complexity, air pollution cannot be addressed by reducing emissions from a single source, but rather by reducing emissions from all sources simultaneously. Furthermore, most air pollution problems cannot be addressed with immediate or quick steps; consequently, a continuous and comprehensive approach, supported by systematic measures, is required, with outcomes expected in the foreseeable future, based on the positive experiences of other countries.

Utilizing experiences and examples from communities that have achieved noticeable improvements is an effective strategy. In response to this urgent concern, a committed UNDP project team has compiled a comprehensive dataset highlighting innovative air protection measures worldwide. This program aims to map global air protection solutions, providing access to a diverse range of beneficial activities, policies, or strategies at local and national levels, while showcasing exemplary cases in the battle against air pollution [53].

The Polish city of Krakow, which is regarded as having some of the worst air quality in Europe, is also an excellent example. Today's scenario is entirely different thanks to the city's leadership and citizens' tenacious actions. Krakow has greatly lowered the concentrations of all pollutants and complies with today's ambient air quality standards thanks to a comprehensive program to enhance air quality that offers inhabitants both practical and financial assistance to upgrade their home heating systems [54].

Consequently, the formulation of targeted and comprehensive plans for air quality management, based on contemporary scientific evidence, along with a robust political commitment to their execution, is imperative.

Lessons learned

Lesson No. 1	Solutions available
<p>Construction activities, especially those involving extensive earthworks during the dry season, can significantly impact local ambient air quality and raise average concentrations outside the heating season. Such activities can lead to increased annual averages and contribute to the violation of regulatory limits. Additionally, the resuspension of road dust is a crucial factor that may broaden the influence of local sources over a wider area.</p>	<p>Effective and cost-efficient methods for controlling fugitive dust are widely accessible. Usually, fugitive dust control programs during constructions works involve organisational and technical measures, ranging from regular supervision, fencing, tire washing and simple water spraying, up to sophisticated fog spraying systems that respond to dust generation intensity and wind changes.</p> <p>Mandatory fugitive dust management plans for larger construction projects, along with effective implementation oversight, might substantially reduce ambient particulate matter concentrations, particularly outside the heating season.</p> <p>Notable examples are cited in the UNDP's publication on solutions to air pollution (https://solutions.sdg-innovation-commons.org/en/view/pad?id=7168), as well as in various technical reference documents.</p>
Lesson No. 2	Solutions available
<p>Disturbance of historical deposition in industrial areas can affect elemental composition and expose the recipients to toxic elements deposited throughout industrial activities.</p>	<p>Preliminary risk assessment for any type of works in areas where current or historical industrial activities occurred should be mandatory, as it can facilitate risk mitigation reduction through effective planning and execution of planned works.</p>

References

1. Kavadarci Municipality's 2022-2026 air quality improvement plan, Tehnolab, 2022)
2. Available at the link: <https://en-gb.topographic-map.com/map-tz1mdn/Municipality-of-Kavadarci/>
3. Available at the link: <https://en.climate-data.org/europe/macedonia/kavadarci/kavadarci-34702/#climate-table>
4. MakStat Database, available at the link:
<https://makstat.stat.gov.mk/PXWeb/pxweb/mk/MakStat/>
5. Available at the link: <https://gpk.mk/>
6. Available at the link: https://www.esm.com.mk/?page_id=1862
7. Chen, K., Zhou, L., Chen, X., Bi, J., & Kinney, P. L. (2017). Acute effect of ozone exposure on daily mortality in seven cities of jiangsu province, china: no clear evidence for threshold. *Environmental Research*, 155, 235-241. <https://doi.org/10.1016/j.envres.2017.02.009>
8. Frei, M., Kohno, Y., Wissuwa, M., Makkar, H., & Becker, K. (2011). Negative effects of tropospheric ozone on the feed value of rice straw are mitigated by an ozone tolerance qtl. *Global Change Biology*, 17(7), 2319-2329. <https://doi.org/10.1111/j.1365-2486.2010.02379.x>
9. Davis, D. D. and Decoteau, D. R. (2018). A review: effect of ozone on milkweeds (asclepias spp.) in usa and potential implications for monarch butterflies. *Journal of Agriculture and Environmental Sciences*, 7(2). <https://doi.org/10.15640/jaes.v7n2a16>
10. Available at the link: <https://source-apportionment.jrc.ec.europa.eu/Specieurope/index.aspx>
11. EMEP/EEA air pollutant emission inventory guidebook 2019, EEA Report 13/2019, available at the link: <https://www.eea.europa.eu/en/analysis/publications/emep-eea-guidebook-2019>
12. Pernigotti, D., Belis, C.A., Spanó, L., 2016. SPECIEUROPE: The European data base for PM source profiles. *Atmospheric Pollution Research*, 7 (2), pp. 307-314. DOI: 10.1016/j.apr.2015.10.007
13. Rigaku NEX CG, website: <https://www.rigaku.com/products/edxrf/nexcg>
14. Standard Operating Procedure for PM2.5 Cation Analysis, revision 7, August 2009, Environmental and Industrial Sciences Division RTI International, Research Triangle Park, North Carolina
15. Guo, H., Gu, X., Ma, G., Shi, S., Wang, W., Zuo, X., ... & Zhang, X. (2019). Spatial and temporal variations of air quality and six air pollutants in China during 2015–2017. *Scientific Reports*, 9(1). <https://doi.org/10.1038/s41598-019-50655-6>
16. Thabeth, N. D., Makonese, T., Masekameni, D., & Brouwer, D. (2024). Diurnal and seasonal variations of particulate matter (PM 2.5) at a tailing storage facility and nearby community. <https://doi.org/10.21203/rs.3.rs-3875400/v1>
17. Yorkor, B., Leton, T. G., & Ugbebor, J. N. (2021). Analysis of temporal variations of air pollutant concentrations in ogoni area, niger delta region, nigeria. *Asian Journal of Environment & Ecology*, 63-73. <https://doi.org/10.9734/ajee/2021/v16i430260>
18. Onanuga, K., Daniel, V., Mustapha, A., & Maitera, O. (2024). Seasonal variations assessment of air pollutants of communities in the vicinity of scrap metal recycling industries in ogijo, shagamu south lga, ogun state, sw nigeria. *Asian Journal of Applied Chemistry Research*, 15(1), 37-47.

19. Liu, X., Wei, Y., Liu, X., Zu, L., Wang, B., Wang, S., ... & Zhu, R. (2022). Effects of winter heating on urban black carbon: characteristics, sources and its correlation with meteorological factors. *Atmosphere*, 13(7), 1071. <https://doi.org/10.3390/atmos13071071>
20. Putaud, J.P., Van Dingenen, R., Alaustey, A., Bauer, H., Birmili, W., et al., 2010. A European aerosol phenomenology – 3: physical and chemical characteristics of particulate matter from 60 rural, urban, and kerbside sites across Europe. *Atmos. Environ.* 44, 1308–1320.
21. Source Apportionment Study for Skopje urban area – identification of main sources of ambient air pollution, AMBICON Lab, Goce Delcev University, Stip, North Macedonia
22. Norris, G., R. Duvall, S. Brown, AND S. Bai. EPA Positive Matrix Factorization (PMF) 5.0 Fundamentals and User Guide. U.S. Environmental Protection Agency, Washington, DC, EPA/600/R-14/108 (NTIS PB2015-105147), 2014.
23. Lee E, Chan C.K., Paatero P., (1999). Application of positive matrix factorization in source apportionment of particulate pollutants in Hong Kong. *Atmospheric Environment*, 33, 3201–3212.
24. Polissar A.V., Hopke P.K., Paatero P., Kaufmann Y.J., Hall D.K., Bodhaine B.A., Dutton E.G., Harris J.M., (1999). The aerosol at Barrow, Alaska: long-term trends and source locations. *Atmospheric Environment*, 33, 2441–2458.
25. Sukon Aimanant & Paul J. Ziemann (2013) Development of Spectrophotometric Methods for the Analysis of Functional Groups in Oxidized Organic Aerosol, *Aerosol Science and Technology*, 47:6, 581-591, DOI: 10.1080/02786826.2013.773579
26. Xie Y., Berkowitz C.M., (2006). The use of positive matrix factorization with conditional probability functions in air quality studies: an application to hydrocarbon emissions in Houston, Texas. *Atmospheric Environment*, 40, 3070–3091.
27. Begum B.A., Kim E., Biswas S.K., Hopke P.K., (2004). Investigation of sources of atmospheric aerosol at urban and semi-urban areas in Bangladesh. *Atmospheric Environment*, 38, 3025–3038.
28. Bzdusek P.A., Christensen E.R., Lee C.M., Pakadeesusuk U., Freedman D.C., (2006). PCB congeners and dechlorination in sediments of Lake Hartwell, South Carolina, determined from cores collected in 1987 and 1988. *Environmental Science and Technology*, 40, 109–119.
29. Singh K.P., Malik A., Singh V.K., Sinha S., (2006). Multi-way data analysis of soils irrigated with wastewater. A case study. *Chemometrics and Intelligent Laboratory Systems*, 83, 1-12.
30. Soonthornnonda P., Christensen E.R., (2008). Source apportionment of pollutants and flows of combined sewer wastewater. *Water Research*, 42, 1989–1998.
31. Hopke P.K., (2003). Recent developments in receptor modeling. *Journal of chemometrics*, 17, 255–265.
32. Belis C.A., Favez O., Mircea M., Diapouli E., Manousakas M-I., Vratolis S., Gilardoni S., Paglione M., Decesari S., Mocnik G., Mooibroek D., Salvador P., Takahama S., Vecchi R., Paatero P., European guide on air pollution source apportionment with receptor models - Revised version 2019, EUR 29816 EN, Publications Office of the European Union, Luxembourg, 2019, ISBN 978-92-76-09001-4, doi:10.2760/439106, JRC117306.
33. Polissar, A. V., Hopke, P. K., & Poirot, R. L. (2001). Atmospheric aerosol over Vermont: chemical composition and sources. *Environmental science & technology*, 35(23), 4604–4621. <https://doi.org/10.1021/es0105865>
34. Mirakovski, D., Zendelska, A., Boev, B. et al. Evaluation of PM2.5 Sources in Skopje Urban Area Using Positive Matrix Factorization. *Environ Model Assess* 29, 1–14 (2024). <https://doi.org/10.1007/s10666-024-09961-1>

35. H. Simon, L. Beck, P.V. Bhave, F. Divita, Y. Hsu, D. Luecken, J.D. Mobley, G.A. Pouliot, A. Reff, G. Sarwar, M. Strum, The development and uses of EPA's SPECIATE database, *Atmos. Pollut. Res.* (2010), pp. 196-206, 10.5094/APR.2010.026

36. Zhang, X., Hecobian, A., Zheng, M., Frank, N. H., and Weber, R. J.: Biomass burning impact on PM_{2.5} over the southeastern US during 2007: integrating chemically speciated FRM filter measurements, MODIS fire counts and PMF analysis, *Atmos. Chem. Phys.*, 10, 6839-6853, 10.5194/acp-10-6839-2010, 2010.

37. Lee, S., Liu, W., Wang, Y., Russell, A. G., and Edgerton, 948 E. S.: Source apportionment of PM 2.5: Comparing PMF and CMB results for four ambient monitoring sites in the southeastern United States, *Atmos. Environ.*, 42, 4126-4137, 2008.

38. Duvall, R. M., Majestic, B. J., Shafer, M. M., Chuang, P. Y., Simoneit, 846 B. R. T., and Schauer, J. J.: The water-soluble fraction of carbon, sulfur, and crustal elements in Asian aerosols and Asian soils, *Atmos. Environ.*, 42, 5872-5884, <https://doi.org/10.1016/j.atmosenv.2008.03.028>, 2008.

39. Almeida et al. (2020) Ambient particulate matter source apportionment using receptor modelling in European and Central Asia urban areas, *Environmental Pollution*, Volume 266, Part 3, <https://doi.org/10.1016/j.envpol.2020.115199>

40. Sun, Y., Zhuang, G., Tang, A., Wang, Y., and An, Z.: Chemical Characteristics of PM_{2.5} and PM₁₀ in Haze–Fog Episodes in Beijing, *Environ. Sci. Technol.*, 40, 3148-3155, 10.1021/es051533g, 2006.

41. Zhou, Y., Zheng, N., Luo, L., Zhao, J., Qu, L., Guan, H., Xiao, H., Zhang, Z., Tian, J., and Xiao, H.: Biomass burning related ammonia emissions promoted a self-amplifying loop in the urban environment in Kunming (SW China), *Atmos. Environ.*, 118138, <https://doi.org/10.1016/j.atmosenv.2020.118138>, 2020.

42. Paulot, F., Paynter, D., Ginoux, P., Naik, V., Whitburn, S., Van Damme, M., Clarisse, L., Coheur, P. F., and Horowitz, L. W.: Gas-aerosol partitioning of ammonia in biomass burning plumes: Implications for the interpretation of spaceborne observations of ammonia and the radiative forcing of ammonium nitrate, 44, 8084-8093, <https://doi.org/10.1002/2017GL074215>, 2017.

43. Pant, P., and Harrison, R. M.(2013): Estimation of the contribution of road traffic emissions to particulate matter concentrations from field measurements: A review, *Atmos. Environ.*, 77, 78-97, <https://doi.org/10.1016/j.atmosenv.2013.04.028>.

44. Pant, P., and Harrison, R. M.(2012): Critical review of receptor modelling for particulate matter: a case study of India, *Atmos. Environ.*, 49, 1-12.

45. Grigoratos, T., and Martini, G (2019): Brake wear particle emissions: a review, *Environ. Sci. Pollut. Res.*, 22, 2491-2504, 10.1007/s11356-014-3696-8, 2015.

46. Piscitello, A., Bianco, C., Casasso, A., and Sethi, R.: Non-exhaust traffic emissions: Sources, characterization, and mitigation measures, *Sci. Total Environ.*, 766, 144440, <https://doi.org/10.1016/j.scitotenv.2020.144440>, 2021.

47. Smichowski, P., Gómez, D., Fazzoli, C., and Caroli, S.: Traffic-Related Elements in Airborne Particulate Matter, *Applied Spectroscopy Reviews*, 43, 23-49, 10.1080/05704920701645886, 2007.

48. Duong, T. T. T., and Lee, B.-K.: Determining contamination level of heavy metals in road dust from busy traffic areas with different characteristics, *J. Environ. Manage.*, 92, 554-562, <https://doi.org/10.1016/j.jenvman.2010.09.010>, 2011.

49. Liao, H.T., Chou, C.C.K., Chow, J.C., Watson, J.G., Hopke, P.K., Wu, C.F., (2015). Source and risk apportionment of selectes VOCs and PM_{2.5} species using partially constrained receptor models with multiple time resolution data. *Environ. Pollut.* 205, 121-130.

50. Yu, L., Wang, G., Zhang, R., Zhang, L., Song, Y., Wu, B., Li, X., An, K., and Chu, J. (2013): Characterization and source apportionment of PM_{2.5} in an urban environment in Beijing, *Aerosol Air Qual. Res.*, 13, 574-583, 10.4209/aaqr.2012.07.0192.
51. Zhang, Y., Sun, J., Zhang, X., Shen, X., Wang, T., and Qin, M. (2013): Seasonal characterization of components and size distributions for submicron aerosols in Beijing, *Sci. China Earth Sci.*, 56, 890- 900, 10.1007/s11430-012-4515-z.
52. Paul M Lemieux, Christopher C Lutes, Dawn A Santoanni (2004): Emissions of organic air toxics from open burning: a comprehensive review, *Progress in Energy and Combustion Science*, 30, 1, <https://doi.org/10.1016/j.pecs.2003.08.001>
53. Available at the link: <https://www.undp.org/north-macedonia/blog/scaling-solutions-leveraging-open-data-tackle-air-pollution>
54. Available at the link: https://environment.ec.europa.eu/topics/urban-environment/inspiration/krakow-air-protection_en
55. Guidelines for drafting air quality improvement plan. <http://air.moepp.gov.mk/wp-content/uploads/2017/04/Pravilnik-plan-za-podobravanje-na-kvalitetot-na-vozduhot.pdf>